ADVANCED MATERIALS INTERFACES
www.advmatinterfaces.de

Face to Face at the Cathode Electrolyte Interphase: From Interface Features to Interphase Formation and Dynamics

Sebastian P. Kühn, Kristina Edström, Martin Winter, and Isidora Cekic-Laskovic**

Development of high-performing lithium-based batteries inevitably calls for a profound understanding and elucidation of the reactivity at the electrode–liquid electrolyte interface and its impact on the overall performance and safety. The formation, composition, properties, and mechanisms of the cathode electrolyte interphase (CEI) formation and function are still to a large extent unknown for most lithium-based battery materials, whereas the same is well considered for the solid electrolyte interphase on negative electrodes in the literature. In particular, in high voltage regions >4.3 V, the oxidative stability limit of most liquid electrolytes is reached and new mechanisms, involving surface reactivity of the active material beside electrolyte decomposition, contribute to the interfacial reactivity and nature of the CEI. Focusing on lithium-based cell chemistries, this review aims to highlight the impact of the still less understood electrolyte decomposition chemistry, dictated by the nature of its components, as well as the in-depth research on the physicochemical and electrochemical properties of CEI formation and evolution at positive electrode material surface and sub-surfaces.

1. From Electrochemical Two-Phase (Interface) to Three-Phase (Interphase) Considerations

The central phenomenon of an electrochemical process in an electrochemical device is the transfer of charge at a phase boundary between an electronically conducting phase called electrode and an ionically conducting phase called electrolyte.[1] This phase boundary represents an electrochemical interface as the only "legitimate" site for charge (= electron or ion) exchange in a battery cell and is ultimately responsible for voltage and rate of any electrochemical device. Apart from that, other reactions at this interface are considered as parasitic and are usually irreversible by nature. We will continue with liquid electrolyte Li based chemistries from here on. Mitigating the decomposition reactions of liquid electrolyte formulations is inevitable to control important benchmarks for lithium-based battery cells, for example, overall power, energy, and life performances as well as safety. However, a complex battery cell system is challenging to control, because of a wide variety of cell configurations: different electrolyte formulations and electrode materials go hand in hand with diverse operating parameters and conditions, not allowing for a universally valid understanding of the key reaction mechanisms at the phase boundary.[2–4]

Defined as the distance between the electrode surface and the immediate layer of counter ions of the electrolyte, the thickness of an electrode–electrolyte interface is estimated to be <1 nm and therefore regarded as 2D.[5] Using electrode materials reactive with the electrolyte under specific operation conditions results in the decomposition of electrolyte components in contact with the surfaces of the electrodes made from these materials: As a result of (irreversible) electrolyte decomposition, different solid products, including hardly soluble inorganic lithium salts and various lithium-free and lithium containing organic components, deposit or precipitate on the electrode surfaces as more or less compact coatings at electrode|electrolyte interface (**Figure 1**).[5–8] This deposition/precipitation process, taking place upon the contact between electrode and electrolyte (lithium metal battery (LMB) chemistries) or during the initial cycles (lithium ion battery (LIB) chemistries), leads to films/layers/interphases inhibiting or at least diminishing further decomposition of the electrolyte.

The resulting films built-on chemical and morphological structures (difference in the atomic-level structure of both phases at the interface and in the bulk structures) and cannot be viewed as 2D interfaces, but rather as 3D interphases which thicknesses can scale from a few nanometers (nm) to micrometers (μm).[9] This results in the appearance of two new 2D interfaces as boarders between electrode and interphase as well as between interphase and electrolyte (Figure 1). The component arrangement within the interphase regions are compromises

S. P. Kühn, M. Winter, I. Cekic-Laskovic
Forschungszentrum Jülich GmbH
Helmholtz-Institute Münster (IEK-12)
Corrensstrasse 46, 48149 Münster, Germany
E-mail: i.cekic-laskovic@fz-juelich.de

K. Edström
Uppsala University
Department of Chemistry
Ångström Laboratory
Uppsala University
Box 538, Uppsala 75121, Sweden
E-mail: Kristina.Edstrom@kemi.uu.se

M. Winter
MEET Battery Research Center
University of Münster
Corrensstrasse 46, 48149 Münster, Germany

The ORCID identification number(s) for the author(s) of this article can be found under https://doi.org/10.1002/admi.202102078.

DOI: 10.1002/admi.202102078

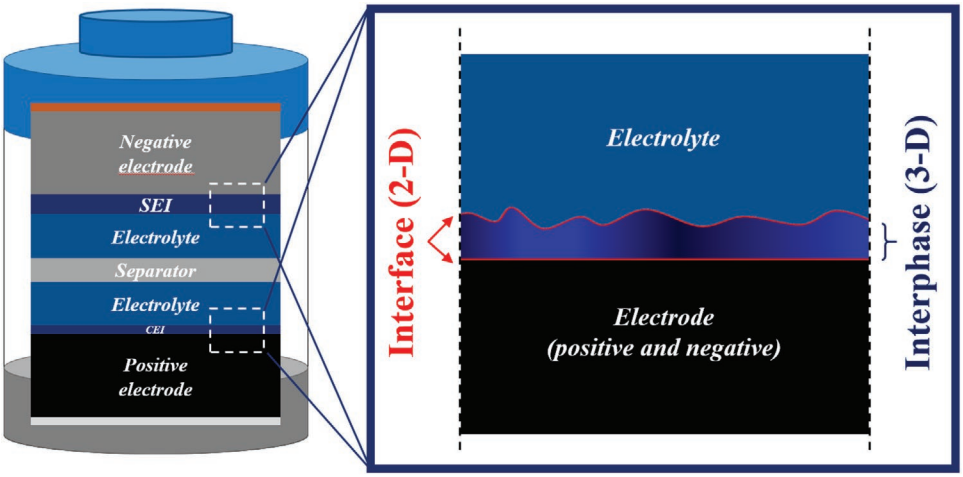

Figure 1. Typical schematic overview of a liquid electrolyte containing battery cell, explicitly depicting the SEI on the negative electrode and the CEI on the positive electrode. The enlarged image illustrates the difference between the 3D structure of the interphase (SEI or CEI) and the 2D boundaries of the electrolyte–interphase interface or the interphase–electrode interface.

between the contradictory demands by both phases. The physicochemical nature of in situ formed interphases is strongly dependent on the liquid electrolyte composition, namely the type of conducting salt, solvents/co-solvents and functional additives.[10] Since the interphases are formed on both electrodes, anode and cathode, they are respectively termed as solid electrolyte interphase (SEI)[11] on the anode side and cathode electrolyte interphase (CEI).[12]They dictate the overall performance (reversibility of redox chemistry at the respective electrodes and kinetics of the cell reactions) as well as safety of the battery cell. According to Xu,[5] interphases are a double-edged sword in respect to sufficient protection on one hand and impeded Li^+ ion transfer on the other, necessitating a compromise to find an optimal balance between the two. Although tremendous research was conducted on design, development, characterization, and elucidation of interphases both from experimental,[6,7,13–23] and theoretical[24–32] aspects, interphases still remain "the most important but least understood component in lithium-based battery cells".[33] The formation mechanism, exact structure, and intra-phase transport properties are still under "realist-idealist debate". In addition, the amount of studies conducted on the CEI remain far behind the ones related to the SEI analogues. Both interphases are built up out of the decomposition products of the two differently composed electrodes with the same electrolyte. When it comes to SEI versus CEI composition, it is clear that the two interphases are different. However, it is still an open question, whether the CEI displays similar physicochemical fundamentals as the SEI on negative electrode. Owing to their sensitive chemical nature, elusive manner of formation and the lack of reliable in situ characterization tools, both SEI and CEI are challenging to study and understand. Characterization of the CEI and identification of its chemical composition are even more challenging: Determining the oxidation potentials which are sufficient to decompose the different electrolyte components on the positive electrode has proven to be more demanding compared to the negative electrode, due to the (electro-)chemical nature of the decomposition reactions, which are very much dependent on the electrolyte composition, cathode material and electrode composition as well as electrode surface area.[6,34,35] Cathode materials are known for their strongly nucleophilic and Lewis basic properties which promote the coordination to the oxygen atoms of electrolyte components (e.g., of ethylene carbonate, (EC)),[36] thus initiating the redox reaction. In general, cathode materials are covered by a native surface film of lithium carbonate (Li_2CO_3) and lithium hydroxide (LiOH), which are formed in the reaction of the transition metal oxides with atmospheric carbon dioxide (CO_2) and moisture (H_2O) during storage and processing.[37–40] The presence of Li_2CO_3-based surface film on transition metal-based oxide positive materials (layered lithium cobalt oxide, spinel-type lithium manganese oxide and layered lithium nickel–cobalt–aluminum and lithium nickel–cobalt–oxides)[41] can also originate from incomplete conversion of the carbonate precursors used for the synthesis of the electrodes active materials. Li_2CO_3 is known to react with common electrolyte conducting salts ($LiPF_6$ and $LiBF_4$).[42–44] Furthermore, oxidation of the state-of-the-art organic carbonate-based electrolyte formulations are usually influenced by the conductive additive in the positive electrode mix alongside the upper cut-off voltage of the battery cell.[45] The decomposition of conventional $LiPF_6$/organic carbonate-based electrolyte starts at voltage >4.5 V.[46–49] An example was published by Rinkel et al., who presented the main organic and inorganic decomposition products as well as the corresponding reaction mechanisms taking place in a $LiCoO_2 \| Li$ cell utilizing an organic carbonate based electrolyte (1 M $LiPF_6$ in EC:DMC 1: (v/v)) at a high stage of charge (SOC) of up to 4.9 V (**Figure 2**).[50] In addition, also anion intercalation into (partially) conductive carbons can take place.[51,52]

2. Electrolyte Stability: Thermodynamic versus Kinetic Approach

While the previous sections focused on the general existence and nature of the 3D interphases, the following section will outline the theoretical physicochemical reasons behind their formation.

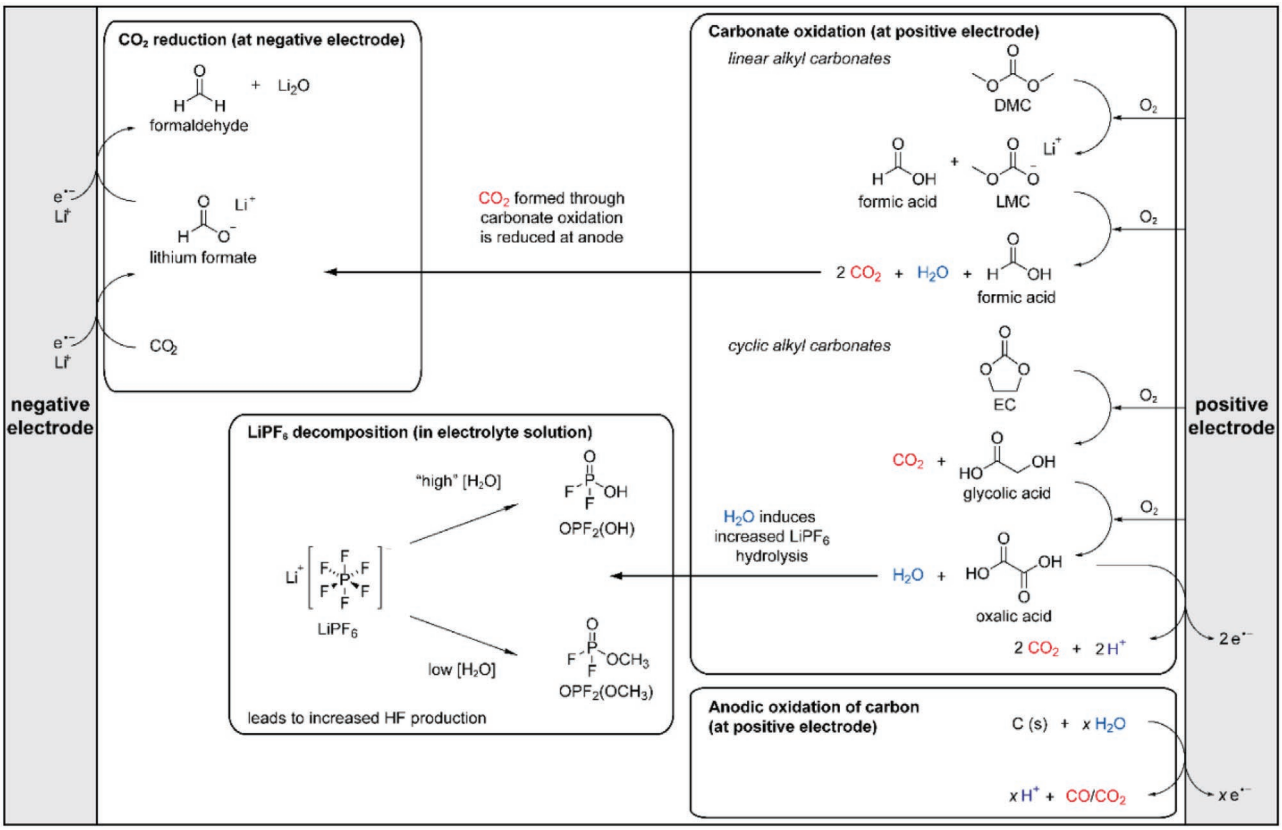

Figure 2. Overview of electrolyte decomposition reactions that occur at high voltage/SOC initiated at the positive electrode. Reproduced with permission.[50] 2020, American Chemical Society.

In LIB, the thermodynamic value of the cell voltage under open circuit voltage (OCV) conditions is determined by the difference between the electrochemical potentials of the anode ($\overline{\mu}_a$) and cathode ($\overline{\mu}_c$). If the value of the anode's electrochemical potential ($\overline{\mu}_a$), lies above the energy level value of the lowest unoccupied molecular orbital (LUMO) of the conventional $LiPF_6$/organic carbonate-based electrolyte, the (in this context) thermodynamic instable electrolyte is reduced on the anode surface. The reduction process continues until the layer well-known as SEI is completely protecting the anode surface, thus inhibiting the electron transfer from the anode to the LUMO of the electrolyte (**Figure 3**a).[53,54] Accordingly, a cathode material with an electrochemical potential ($\overline{\mu}_c$) below the energy level value of the electrolyte's highest occupied molecular orbital (HOMO) leads to the oxidation of the conventional $LiPF_6$/organic carbonate-based electrolyte (Figure 3). The electron transfer from the HOMO to the cathode results in the formation of an effective CEI (Figure 3c). This, in the ideal (desire) case, electronically insulating and well Li^+ ion conducting protective interphase prevents the direct contact of liquid electrolyte and the reactive electrode surface. To overcome the challenges associated with the electrolyte's instabilities at the initial cathode–electrolyte interface, especially during high-voltage (HV) application, two approaches are intensively followed in the literature. The first one comprises development of electrolytes, whose HOMO energy level lies well below the electrochemical potential of the cathode, thus providing an intrinsic thermodynamic stability (Figure 3b).[14,54–58] The second approach relates to the introduction of CEI forming electrolyte additives, electrode surface coatings and pre-assembly modifications of the cathode surface, as an economical and effective approach to rapidly achieve kinetic stability at the interface from the beginning of operation. Cathode surface coatings reduce the parasitic reactions between the cathode material and the electrolyte and therefore already result in a higher Coulombic efficiency during the initial cycles. CEI forming additives, on the other hand, are designed to get preferably oxidized and form an effective CEI on the cathode surface prior to electrochemical oxidation of the bulk electrolyte.[59–67]

2.1. Oxidative Electrolyte Decomposition Pathways

A common approach to raise the energy of battery cells is the increase of the upper cut-off voltage during charge (>4.3 V), which in turn does result in higher operational discharge voltages and frequently also in higher discharge capacities.[68,69] However, electrolyte instability as well as cathode surface reactivity can cause gas evolution and concomitant permanent loss of lattice oxygen as well as degradation and reconstruction of the CEI and transition metal dissolution, which can all be detrimental to the battery cell performance and lifetime.[70–74]

The study of electrochemical stability window as well as of pathways of electrolyte decomposition outside of this window, is

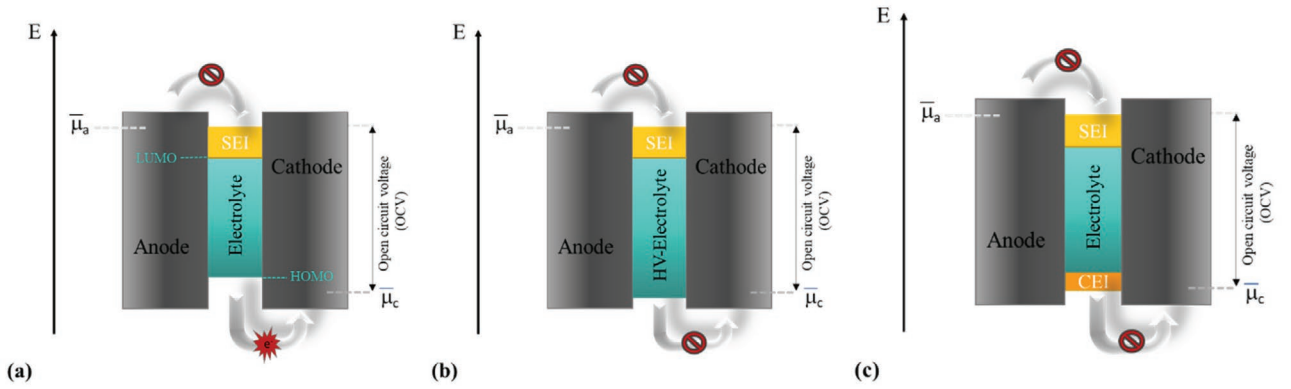

Figure 3. Schematic illustration of LIB energy diagram under open circuit conditions of a battery cathode cell containing: a) $LiPF_6$/organic carbonate-based electrolyte under continuous electrolyte oxidation, b) high voltage stable electrolyte with intrinsic thermodynamic stability, and c) film forming electrolyte additive enabling formation of an effective CEI.

particularly important for design and development of advanced battery materials and cells.[75] Electrolyte decomposition pathways can be categorized into three types of reactions:[76] i) chemical (non-Faradaic) reduction and oxidation, ii) electrochemical (Faradaic) reduction and oxidation, and iii) non-redox reactions, for instance acid-base reactions.

The aforementioned reactions can occur in competition and/or in subsequence o impacting the type and number of components formed as part of the interphase layer, in this case the CEI. For certain cell chemistries, chemical oxidation is the dominant decomposition process, thus intrinsically linking the surface reactivity of the positive electrode and the electrolyte reactions taking place, especially at high cut-off voltage (higher SOC).[50,77] **Figure 4** depicts the main oxidation reactions for organic species (RX) taking place in an electrochemical system and provides starting methods/techniques for identification of intermediate and product species within different reaction mechanisms.[76]

Electrolyte decomposition processes of organic solvent-based electrolytes usually involve solvent/co-solvent and conducting salt anion, thus calling for explicit analysis and understanding of coupling of their decomposition reactions.[77–79] Various reaction mechanisms for organic carbonate-based electrolyte oxidation have been proposed in literature, such as nucleophilic substitution between metal oxide cathodes and organic carbonate molecules,[80–82] electrophilic[83,84] mechanisms and dehydrogenation reactions, including EC dissociation[75] and dissociation with oxygen vacancy formation.[83] One example is the proposed mechanism by Zhang et al. of the oxidative decomposition of 1 M $LiPF_6$ in EMC/EC electrolyte on layered Ni-rich metal oxide positive electrodes (**Figure 5**): The study correlated the decomposition species, identified via in situ FTIR experiments, and their contribution to the CEI impedance growth and capacity loss. The determination of those mechanisms is a vital part in the ongoing quest to deliberately design tailored electrolyte formulations and synthesis of functional additives.

3. Effect of Electrolyte Additive Promoted CEI Formation

Knowledge gained over the last decades has enabled researchers to develop a set of semi-empirical disciplines to tailor interphases. The introduction of sacrificial electrolyte components (functional additives) is regarded as the most effective and cost affordable approach since their amount is usually kept ≤ 5% of the electrolyte composition.[86] An ideal CEI forming additive should fulfill a set of the following requirements: i) lower

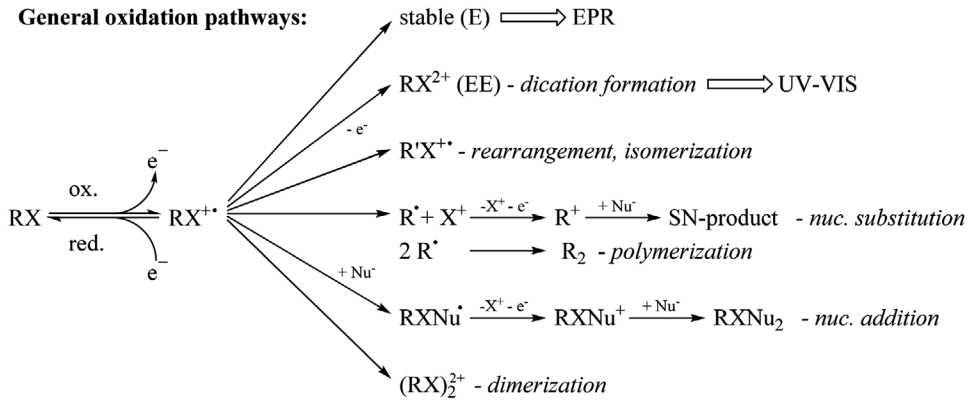

Figure 4. Schematic representation of possible oxidative reaction pathways following initial oxidation of species (RX) in an electrochemical system; R-hydrocarbon; X-substituent.[76]

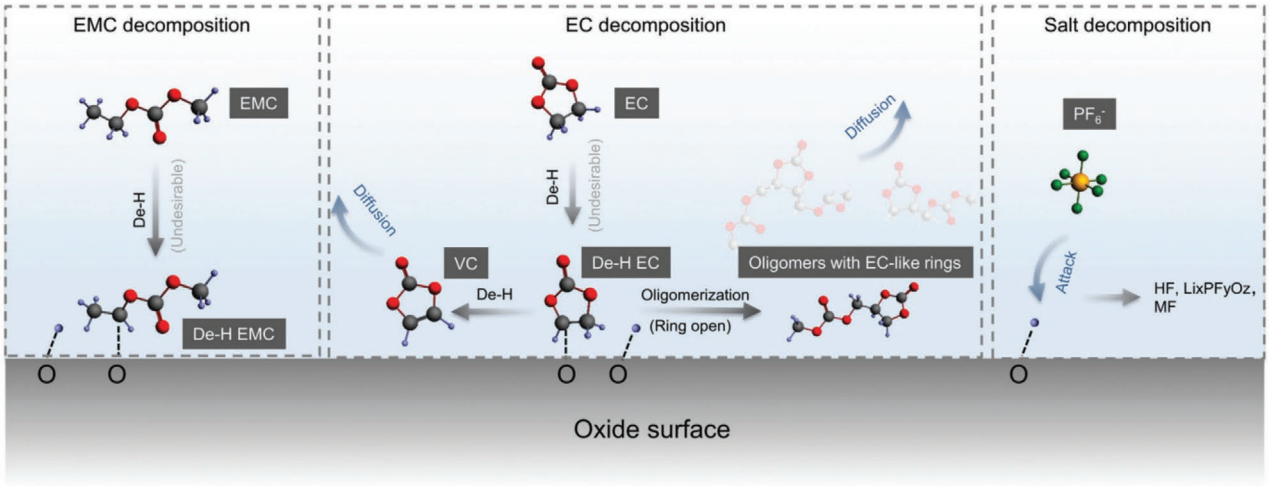

Figure 5. Proposed mechanism and pathways of electrolyte decompositions on NMC811. Electrolyte decomposition reactions include solvent (EMC and EC) decomposition and coupled salt (PF_6^-) decomposition. Solvent decomposition happens by dehydrogenation first, and de-H EC could be further decomposed by removal of another hydrogen or by oligomerization. The protic species at the interface coming from dehydrogenation could further attack PF_6^- and lead to coupled salt decomposition. The decomposed species (mainly solvent decomposed species) would form a resistive layer at the interface and lead to large impedance growth, eventually resulting in capacity loss for NMC811. Reproduced under the terms of the CC-BY 3.0 license.[85] 2020, The Authors, published by The Royal Society of Chemistry.

oxidation potential than state of the art (SOTA) electrolyte components, ii) compatibility with SOTA electrolyte components, iii) compatibility with the anode, and iv) enhancement of the ionic conductivity.[55,87,88] There are many compounds that can fulfill the requirements considering the compatibility with the SOTA electrolyte components and the negative electrode, however, a most crucial requirement refers to the lower oxidation potential compared to the SOTA electrolyte. Many different CEI additives are known in literature, which can be categorized according to their molecular structure and further divided with regard to the containing elements (**Figure 6**).

Fluorinated organic molecules are the largest and most investigated group of functional additives and can be divided further depending on the utilized heteroatoms.[66,89–113] The two other groups of potential additives for high-voltage applications are organic metal-based[67,90] and lithium salt-based[114–121] molecules. All these additives decompose prior to the SOTA electrolyte and form an effective CEI. However, not every formed CEI is an ideal compromise, which fulfills all of the following requirements: i) facilitate (or at least does not impede) lithium ion transfer, ii) reduce the interfacial/interphasial resistance, iii) reduce transition metal dissolution, iv) suppress gas generation, v) prevent structural changes of the electrode active material, and vi) prevent side reactions between the electrolyte formulation and the electrode (**Figure 7**).[89,93,94,98,99,104,109,119,122–129]

3.1. The Role of Fluorine in CEI Film Forming Additives

Since F is a most utilized compound for high-performance applications, it is worth to take a stronger look at its chemistry: Fluorine can form chemical compounds with hydrogen, metals, nonmetals, even noble gases, and a diverse set of organic compounds. With an adopted oxidation state of –I, the fluoride-ion forms a great variety of chemical compounds by either polar covalent or ionic bonds. An additional merit of fluorine containing additives as part of an electrolyte is their tendency to combust rather than to catch fire.[130] Fluorinated electrolytes have been demonstrated to help reaching new levels of performance and safety in high voltage batteries.[131–137] In case of high voltage application, the substitution of hydrogen with fluorine atoms leads to reduced activation energy[138] and decreased HOMO and LUMO energy levels, thus resulting in increased reduction and decreased oxidation potentials.[12,95,133,139–141] In most cases, this decreased HOMO energy level leads to improved cycling performance which is related to the early formation of an effective CEI layer as well as to the decreased overall impedance.[95,133,139,142] There are numerous publications in the recent years featuring fluorinated high voltage additives.[86,113,143–154] However, in most cases the authors do not clarify whether fluorination is essential for the additive performance for high voltage batteries or not. Therefore, further profound understanding of the fluorine atom's impact on the overall performance of lithium-based cell chemistry has to be the topic of future research, including: i) finding correlation between the molecular and electronic structures of fluorinated electrolyte components, ii) identifying relevant physicochemical properties and reactivity, iii) revealing synergistic effects between fluorinated and non-fluorinated electrolyte components, iv) elucidating main operation and failure processes in the lithium-based cell, v) studying of different plausible reaction pathways, and vi) analysis of the limiting and determining steps which provide rationalization of the obtained results. This research as well as the integration of gained knowledge comprising the aforementioned parameters and processes is key toward desired advancements of lithium-based cell chemistries and their effective performance (**Figure 8**).[133,154]

The formation, thickness, dynamics, and morphology of the CEI are dependent on the nature and properties of the considered electrolyte and, therefore, research regarding the

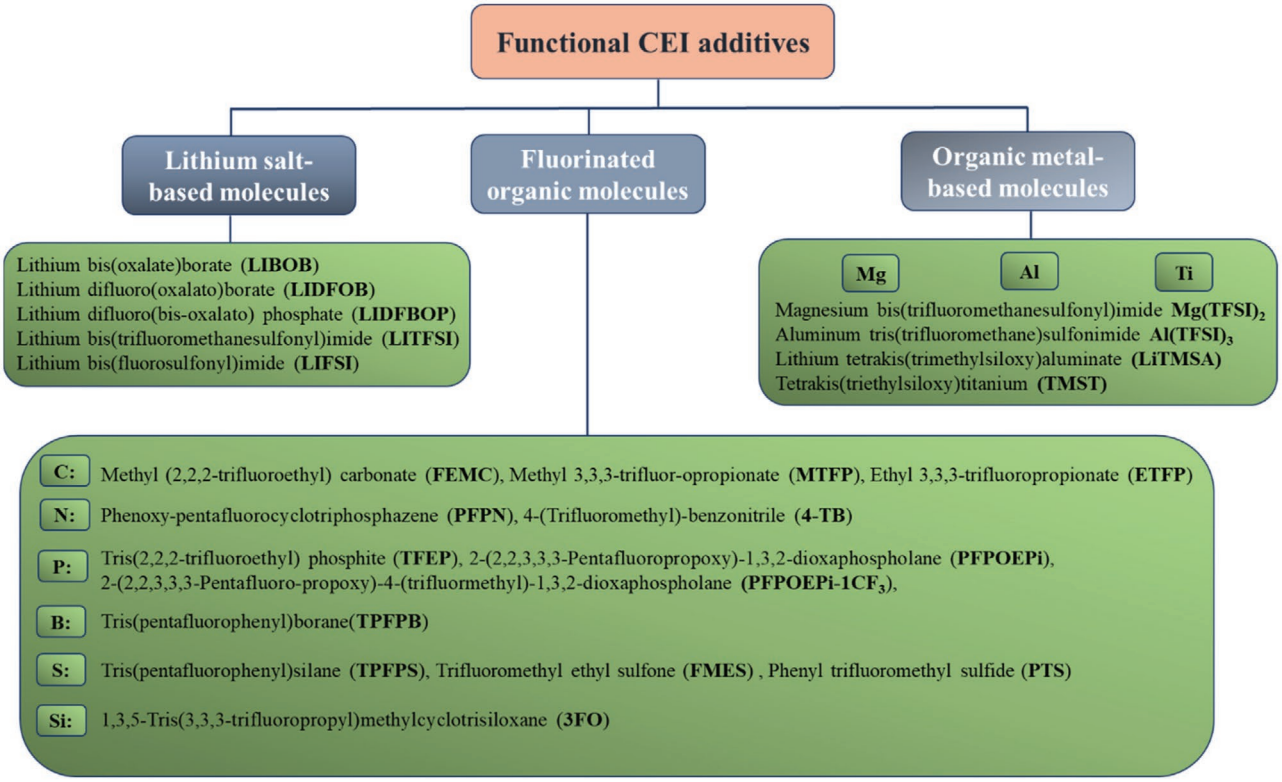

Figure 6. Overview of the different classes of functional CEI additives, sorted depending on their molecular structure and presence of heteroatoms, given with common representatives.

structure-property-performance-relationship is essential to understand the impact of the different electrolyte compounds on the CEI formation. An additional point, still in the stage of repeated experiments and exploration, addresses the question how to properly combine multiple electrolyte additive(s), that they do fulfill the different of cathode requirements. In some cases, single additive utilization fails to meet the requirements in respect to formation of an effective CEI layer that can protect the cathode and can prevent the increase of total battery impedance. In this respect, design and development of multifunctional additives or mixtures of at least two carefully selected functional additives seems to be a more effective approach.[130,149,155–158]

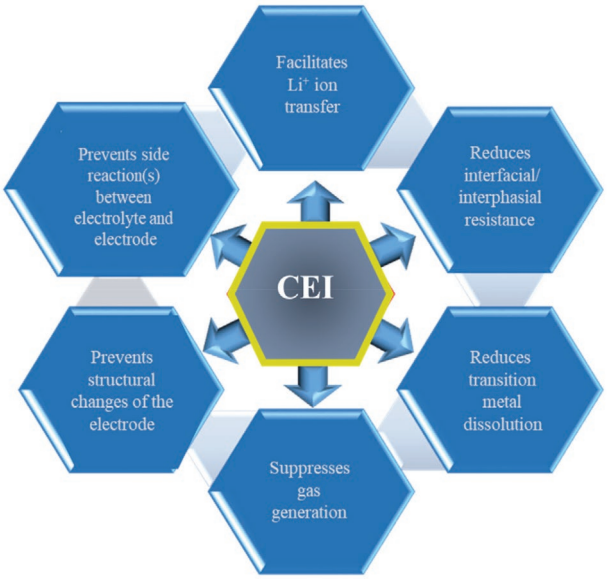

Figure 7. Set of requirements for an ideal CEI.

4. Formation and Evolution of the CEI

Most of the reviewed studies up to this point have dealt with theoretical studies or proposed mechanisms on CEI formation and the overall performance enhancing effect of an effective CEI for advanced batteries. They reported on the CEI's strong dependency on the type of cathode material[15,16,159,160] the inactive materials in the composite electrode[161] and the electrolyte formulation.[162] However, detailed studies of the CEI formation and evolution, ideally utilizing operando and/or high-precision analysis methods, are not as frequent and have only been reviewed on a small scale.[20] Therefor, the increased amount of publications of the stated variety in the last few years will be reviewed in the coming sections, as well as other research of the same topic, utilizing more common ex situ analysis methods. Hopefully this review will lead to more interest in this specific field of research, since a is the foundation for future improvements of all types of cathode-based battery systems.

The CEI and the battery cell performance is influenced by a large variety of different factor configurations, comprising among others: cathode electrode composition, electrolyte,

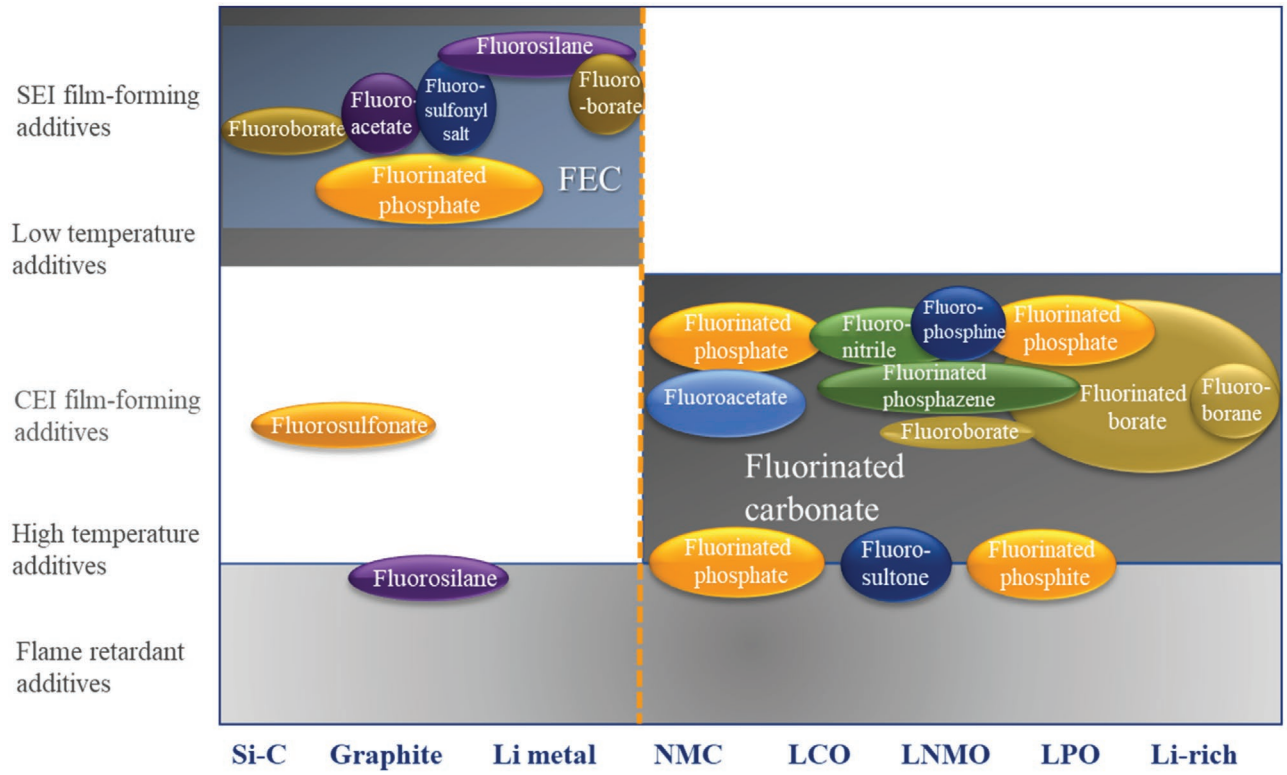

Figure 8. Summary of the types and applications of fluorinated additives in lithium ion batteries. Reproduced with permission.[154] 2020, Elsevier.

anode material, and cell potential. A condensed overview of the respective cathode and anode materials as well as the electrolyte formulation and analysis methods of the reviewed studies in the next sections are summarized in **Table 1**. The influence of different anode materials on the CEI will get touched on in a separate CEI-SEI crosstalk section. The wide variety of different cell configurations in comparison to the limited number of publications, already shows the need for more systematic research to paint a clearer picture of the CEI formation and its evolution depending on the different cell configurations.

4.1. Formation

The first step in the lifetime of a CEI layer is its formation during the initial charge and discharge steps of the battery cell. The SOC has been stated on multiple occasions as an highly influential factor for the CEI:[50,77] Depending, on different starting SOC, different self-discharge currents have been observed as the result of electrolyte decomposition utilizing a "high precision electrochemical measurement device".[36] Density function theory (DFT) supported those findings and determined EC as the main component of parasitic reactions at the surface of cobalt atoms, initiated by the coordination of EC's oxygen atom and a cathode's cobalt atom.[167] As a counter reaction, 2D-Raman analysis was able to show the stepwise oxidation of the cathode's cobalt atom to Co_3O_4 and finally Co_2O_3, which becomes part of the CEI.[163] Those in detail analyses draw two conclusions: i) combining different characterization and modeling methods is the way to go to get a clearer picture of EI formation and evolution and ii) only detailed analyses can result in tailored solutions for given problems. In this case it was shown that the conjugation of silane or cyanide containing electrolyte additives to those exposed cobalt sites can reduce the EC decomposition and thereby increase the initial capacity retention of the above cell configuration.[36,167]

In another study, Scipioni et al. introduced atomic probe tomography (APT) in combination with electron impedance spectroscopy (EIS) measurements to investigate the CEI on $LiMn_2O_4$ under OCV conditions. A layered structure of the CEI (**Figure 9**) was found, with the inner layer predominantly contains fluorinated manganese species. Those form during the initial 24 h of OCV and result in an increase in charged transfer resistance. The interfacial CEI resistance (R_{CEI}) experiences a further increase over the following hours in OCV, which is attributed to the formation of an outer CEI layer containing various organic and inorganic compounds.[164] This detailed analysis method seems to be very promising, as it results in an accurate depiction of the CEI and its formation time. This study shows that the CEI formation has different stages: Initial formation during OCV and further electrochemical formation during cycling. So far, there are only a few other studies known in the literature regarding the layered structure of the CEI,[165] which consequentially demands additional and more profound in depth research on the detailed component distribution within the CEI.

Another high precision method which has revolutionized other chemistry research areas, like structural

Table 1. CEI formation and evolution research overview: battery cell configuration (active materials, electrolyte formulation) and utilized analysis method (i.s. = in situ; i.o. = in operando).

Cathode	Electrolyte	Anode	Analysis method
$LiCoO_2$[36]	–	Li metal	Self-discharge, DFT
$LiCoO_2$[163]	1 M $LiPF_6$, EC/DEC 1:1 v/v	Li metal	2D Raman
$LiMn_2O_4$[164]	1 M $LiPF_6$, EC/DMC 1:1 v/v	Li metal	APT, EIS
NMC811[165]	1 M LiPF6 or 1 M LiDFOB in EC/DMC/EMC 1:1:1 (v/v/v)	Li metal	XPS, EIS
Li/Mn-rich NMC[166]	1 M $LiPF_6$, EC/DEC 1:1 v/v	Li metal	cryo-EM, TEM
NMC811, LMNO[167]	1 M $LiPF_6$, EC/EMC 1:2 v/v	–	i.o. ATR-FTIR, XPS, HRTEM
$Li_{1.2}Ni_{0.12}Co_{0.12}Mn_{0.56}O_2$[168]	1 M $LiPF_6$, EC/DEC 1:1 v/v	Li metal	i.s. EQCM, CV, EIS
NMC811[169]	1 M $LiPF_6$, EC/DEC 3:7 w/w	Li metal	HAXPS, SAXS, DFT
$LiCoO_2$[170]	1 M LiPF6 EC/DMC/EMC 1:1:1 (v/v/v)	Li metal	i.s. AFM
LR-NMC, LRMO, LNMO[171]	1 M $LiPF_6$, EC/DMC 1:1 v/v	Li metal	XPS
$LiMn_{1.5}Ni_{0.5}O_4$, $Li_{1.2}Mn_{0.6}Ni_{0.2}O_2$, $LiNi_{0.94}Co_{0.06}O_2$[172]	1 M $LiPF_6$, EC/EMC 3:7 w/w	Li metal	TOF-SIMS
LNMO[173]	1 M $LiPF_6$, EC/EMC 1:1 v/v	Li metal	TOF-SIMS, XPS
LNMO[174]	1.3 M $LiPF_6$, EC/EMC/DEC 3:2:5 (v/v/v)	Li metal	XPS EIS
NMC811[175]	1 M $LiPF_6$, EC/EMC 3:7 v/v +1 wt% VC	Li metal	TEM, XPS, EIS
NMC111[176]	1 M $LiPF_6$, EC/EMC 3:7 w/w + 2 vol% FEC, VC, ES	Li metal	XPS, SEM, GC-MS
NMC532[177]	1 M LiPF6 EC/DMC/PC 1:3:1 (v/v/v)	Li Metal	XPS, SEM
$LiCoO_2$[178]	1 M $LiPF_6$, EC/DMC 1:1 v/v	Li metal, graphite	XPS
NMC532[179]	1 M $LiPF_6$, EC/DEC 1:1 v/v	Li metal, graphite, lithium titanate	XPS
$LiRu_2O_3$[180]	1 M $LiPF_6$, EC/DMC 1:1 v/v +10 wt% FEC	Li metal	SSNMR, DNP, EIS
$LiCoPO_4$[181]	1 M $LiPF_6$, EC/DMC 1:1 v/v	Li metal	HIM, i.s. TOF-SIMS
NMC622 (Cr_2O_3/TiO_2/ZnO coated)[182]	1.2 M $LiPF_6$, EC/EMC 3:7 w/w	Li metal	EIS, XPS
NMC811[183]	1.4 M LiFSI, DMC/EC/TTE 2:0.2:3 n/n	Graphite	XPS, HRTEM
NMC532[184]	2 M LiTFSI/LiDFOB, TMS/EA 3:7 v/v + HFE	Li metal	XPS, TEM
NMC532[185]	4 M LiFSI, DME + HFE	Li metal	XPS, TEM
Layered-NMC60535[186]	1.5 mol kg^{-1} $LiPF_6$ EMC/DMC, 9:1 w/w + 15 wt% FEC, 1 wt% VC, 0.5 wt% LiDFOP	Li metal	SEM, HRTEM, EIS
layered-$Li_2Ni_{0.94}Co_{0.06}O_2$[187]	1.5 M $LiPF_6$, EMC + 3% VC	Graphite	TOF-SIMS +^{6}Li labeling
NMC811[188]	1 M $LiPF_6$, MTFP/FEC 9:1 v/v	Li metal	XPS
$LiMn_{1.5}Ni_{0.5}O_4$[189]	1.0 M LiPF 6, EC/DEC + ETFEC	Li metal	SEM, TEM, XPS
$LiNiO_2$[190]	1 M/sat. $LiNO_3$ + LiOH	Graphite	XPS, TEM
$LiMn_2O_4$[191]	21 M LiTFSI, 7 M LiOTf in H_2O	Graphite	XPS, SECM
V_2O_5[192]	1 M KPF_6/PC	K metal	i.s. XAS, XPS, TEM, Raman

biochemistry,[193,194] is cryo-electron microscopy (cryo-EM). Zhang et al. combined this method with transmission electron microscopy (TEM) to investigate the CEI on a nanometer scale. Their findings show no uniform passivation layer covering different lithium and manganese rich NMC cathode materials which will also not form in an OCV or during prolonged cell runtime. A homogeneous CEI was only formed in situ upon shortening the cell externally for 20 s, forcing extensive electrolyte decomposition on the cathode surface. In situ CEI formation resulted in an increased capacity retention of +81% after 100 charge/discharge cycles at 0.5C.[166] Since the CEI's nature is very fragile, and therefore has to be handled with extreme care to not be contaminated or altered during ex situ/post mortem analysis. Therefore, the challenging investigation of an untouched CEI within the confines of the cell, should be the way for CEI research going forward. In situ-FTIR experiments were already used to investigate the oxidative decomposition of electrolytes in the cathode surface.[85] The attenuated total reflection–Fourier transform infrared (ATR-FTIR) technique was then used as an operando method to investigate the CEI on $LiMn_{0.8}Ni_{0.1}Co_{0.1}O_2$ (NMC811)[195] and $LiMn_xNi_{1-x}O_2$ (LMNO)[167] cathode materials. Meng et al. were able to report the priority decomposition of EC on the LMNO cathode surface during a charge and discharge process. Based on the experimental results it was concluded, that the CEI on a lithium rich LNMO cathode ($Li_{1.2}Ni_{0.2}Mn_{0.6}O_2$) is predominantly build up during the first charge and discharge step, and experiences a dynamic evolution during the following cycles. They also used X-ray photoelectron spectroscopy (XPS) and high resolution TEM (HRTEM) measurements to investigate the film forming tendencies of the silane-based additive tris(trimethylsilyl)-borate.[167] XPS measurements are still the most common method to attempt the challenging determination

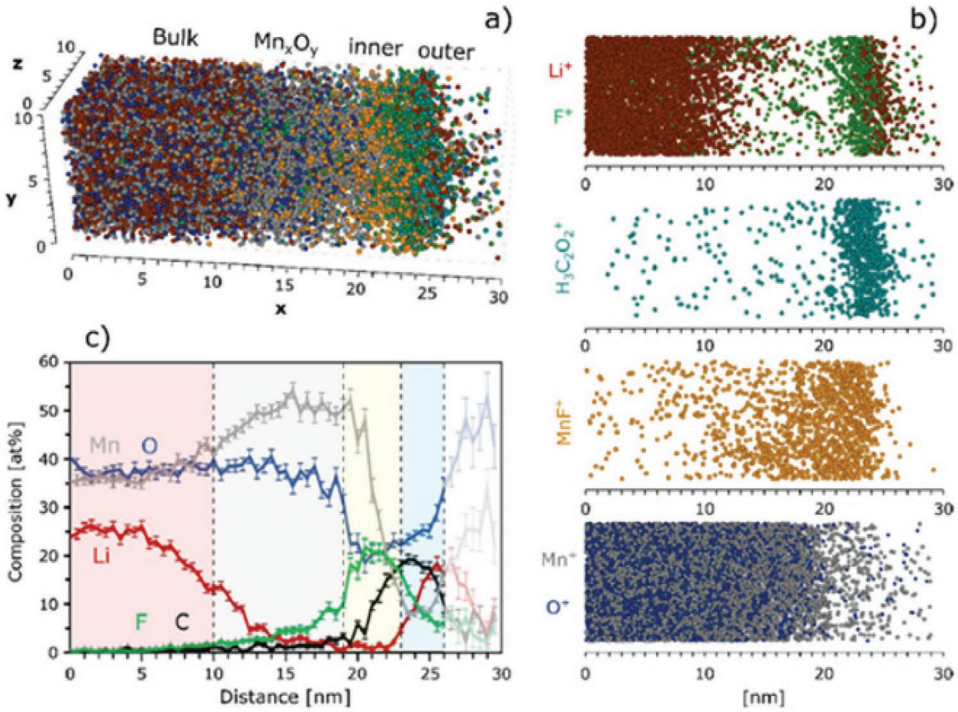

Figure 9. Atomic resolution analysis of the CEI. a) 3D APT ion map b) 2D projections, normal to the *x*–*y* plane, of the single ion maps for Li^+, F^+, $H_3C_2O_2^+$, MnF^+, Mn^+, and O^+ c) Composition profiles of the atomic fractions for Li, Mn, O, F, and C. The colored regions in c) are meant to approximately indicate four regions, from left to right: 1) the LMO electrode bulk, 2) a Mn_xO_y layer on the electrode surface and the CEI layer composed of 3) an inner homogeneous MnF_x layer, and 4) an outer mosaic-structured layer. Note that the atomic composition calculated in the last 4 nanometers of the 3D ion map is not considered meaningful, because of the small number of ions detected in this region. Reproduced with permission.[164] 2020, Elsevier.

of the chemical compositions present in the CEI. However, "normal" XPS has its limitations, which can be compensated by more refined spectroscopy and/or a combination of different investigation methods. Takahashi et al. used hard X-ray photoelectron spectroscopy (HAXPES), soft X-ray absorption spectroscopy (SAXS), and DFT calculations to investigate the CEI on the nickel rich cathode material NMC811 ($LiNi_{0.8}Mn_{0.1}Co_{0.1}O_2$). They found that the CEI mostly contains inorganic lithium-containing electrolyte decomposition products like $LiCO_3$ and $LiPO_xF_y$. Compared to so-called lithium rich cathode materials,[196] the cause for the ever-increasing growth of the CEI was proposed to be the very low energy gap between the LUMO of the cathode material, especially of nickel vacancies in the atomic structure, and the HOMO of the electrolyte.[169]

After the determination of the CEI's chemical composition and the determination of a high SOC as main driving force behind CEI formation, the next question is about the exact voltage levels during charge and discharge, which result in electrolyte decomposition: For the lithium rich NMC cathode material ($Li_{1.2}Ni_{0.12}Co_{0.12}Mn_{0.56}O_2$ = $0.5\ Li_2MnO_3 \cdot 0.5\ LiNi_{0.3}Co_{0.3}Mn_{0.4}O_2$), this was determined by Yin et al., who used a combination of in situ electrochemical quartz crystal microbalance (EQCM), cyclic voltammetry (CV) and EIS measurements to investigate the processes on the cathodes surface during the first charge/discharge cycle in the voltage range up to 4.8 V. It was found that during the initial charge cycle the native CEI layer is dissociated up to 4.4 V before a new electrolyte combustion based CEI layer is formed between 4.4 and 4.65 V. This initial CEI is than again reinforced during the first discharge cycle in the voltage range from 4.1 to 2.6 V.[168]

Multiple cited publications already mention inhomogeneous CEI formation on the cathode surface, predominantly induced by an inhomogeneous reactivity on the cathode surface.[166,169] In situ AFM measurements were performed by Lu et al. to find the sites of CEI formations on $LiCoO_2$ cathodes: At high SOC, CEI formation predominantly happens on the edge plane of the cathode material, and almost no interphase formation happens on its basal plane. They also reported on the inhabitation of the CEI formation on either plane by coating the cathode material with two runs of atomic layer deposition of Al_2O_3.[170]

Even though all above publications investigate different factor configurations, following conclusions can be drawn for the initial CEI formation: i) CEI formation happens predominantly at the sight of uncovered transition metal atoms.[36,169,170] ii) EC is the initial decomposed component of organic carbonate-based electrolytes on the cathode surface.[36,167] iii) The CEI formation is promoted at high cell potentials due to an increased electrolyte decomposition.[36,168–170] iv) Different transition metal coordinating additives and cathode coatings can inhibit the electrolyte decomposition on the cathode surface.[36,167,170]

4.2. Evolution

CEI formation and evolution are correlated processes, however, whereas formation happens during the first cycles, the

following paragraphs will focus on CEI evolution, which is predominantly influenced by electrochemical processes. Even though operando analysis tools have to be the preferred strategy for future CEI evolution investigations, great scientific results have been published in this field of research using ex situ/post mortem analysis. XPS,[171,173–176,178,179,182,190–192,197] EIS,[174,175,180,182] and time-of-flight secondary ion mass spectrometry (TOF-SIMS)[172,173,181] are widely utilized methods, often in combination or with other complimentary methods.

Li et al. used (depth profile) XPS surface measurements to investigate the CEI composition and thickness on various structurally different cathode materials (layered lithium rich NMC (LR-NMC) and $LiRu_{0.5}Mn_{0.5}O_2$ (LRMO) and spinel LMNO) in a charged and discharged state. They found that spinel structured cathodes are less likely to form a thick CEI layer of organic carbonate-based electrolyte decomposition products and that Ru as part of LRMO promotes a thicker CEI formation, as well.[171] In a different study, Erikson et al. used TOF-SIMS to investigate the CEI on two LMNO spinel cathodes ($LiMn_{1.5}Ni_{0.5}O_4$, $Li_{1.2}Mn_{0.6}Ni_{0.2}O_2$) and one ultra-low cobalt cathode material ($LiNi_{0.94}Co_{0.06}O_2$). It was reported that the CEI on all three cathode materials are covered by a carbonate and hydroxyl based CEI from the beginning, which experiences a dynamic change of chemical composition due to constant electrolyte combustion, especially at high voltage values.[172] Furthermore, Wu et al. also used TOF-SIMS, in combination with XPS, to investigate lithium and manganese rich LMNO cathode materials, and reported a rather inhomogeneous and non-uniform CEI coverage on the pristine material after long term cycling.[173] Those results once more showed, the significant influence of the cathode material on the CEI's nature, both during formation and during evolution.

The different chemical reactions on the cathode surface, which result in the desired formation and repair of the CEI, also results in by-products, which, have to be taken care of to not have a detrimental effect on the battery cell. The most investigated of those electrolyte decomposition products is hydrofluoric acid (HF) and different other fluorophosphates:[173,174] Important CEI components like lithium fluoride (LiF) and different lithium fluorophosphates ($LiPO_xF_y$) are easily "leached out"[174] of the CEI, destabilizing it, which consequentially leads to even more electrolyte consumption and the start of a self-promoting degradation cycle. The incorporation of a lithium phosphate (Li_3PO_4)[173] as a cathode doping agent as well as cathode coating with aluminum oxide (Al_2O_3) or copper oxide (CuO)[174] were able to inhibit this self-promoting cycle. In case of Al_2O_3 and CuO the pH value of the electrolyte was kept at a constant value, which is caused by the HF-scavenging effects of the metal oxide coatings.

Alongside these harming effects taking place at the electrolyte–CEI interface, there are also cathode sided degradation processes which can damage the integrity of the CEI. One observed example was reported by Wang et al., who investigated the CEI evolution on NMC811 under high voltage conditions (4.6 V, 4.9 V) using TEM, XPS, and EIS experiments. Upon extended cycling to high cut-off voltages, an additional transition phase is formed within the confines of the CEI interphase on the cathode material surface containing spinel and cubic structures (**Figure 10**). These new structures increase the effective cathode surface, putting the CEI under mechanical stress, which promotes CEI cracking,[175] and

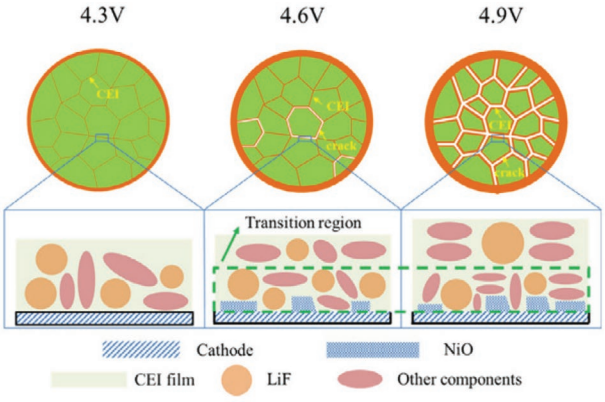

Figure 10. Illustration of the NCM811 cathode surface after 50 cycles under different conditions. Reproduced with permission.[175] 2019, Elsevier.

would once again cause the start of the aforementioned self-promoted degradation cycle.

This problem of a cracking interphase is rather similar to the one of the SEI on lithium metal anodes and functional additives have been the go to approach to circumvent those problems on the anode surface.[8,198–200] However, there are limited publications, which compare different additives and their influence on the CEI in the same cell factor configuration.[176,177] Qian et al. investigated the influence of three commonly used functional additives (fluoroethylene carbonate (FEC), vinylene carbonate (VC), ethylene sulfite (ES)) in organic carbonate-based electrolytes on the CEI of a NMC111 cathode. Quantitative and depth profiling XPS analysis as well as SEM and GC-MS analysis in combination with galvanostatic cycling were the analytical tools for this study. A correlation was found between the best performing FEC additive for galvanostatic cycling and the constantly thin CEI, which contained LiF as the main component. FEC passivated cathodes, contrary to VC and ES passivated cathodes, also experienced the lowest degradation and thereby the fewest additional electrolyte consumption, once more underlining the effectiveness of fluorine containing functional additives.[176] Different amounts of the used additive can also have an influence on the CEI, for example, varying higher amounts of FEC can result in an increased thickness of the CEI on $LiNi_{0.5}Mn_{1.5}O_4$ electrodes.[197]

In summary, the application of operando analysis has not yet found its way into the investigation of the CEI evolution on a longer time scale. For now, results of ex situ/post mortem analysis have to be the source for a few initial conclusions: i) Different cathode materials show different tendencies for the formation of the CEI[171–173] and, in all reported cases, repeated charging to high cut-off voltages decreases the battery lifetime, which is mostly caused by ongoing electrolyte decomposition.[172,175] ii) This is the result of constant degradation and subsequent rebuild of the CEI during each charge/discharge cycle, induced by the formation of new transition metal-based substructures within the CEI[175] as well as the highly reactive electrolyte decomposition product HF.[173,174,201] iii) This self-promoting degradation cycle can be inhibited by functional additives, cathode doping or coating, either by forming an effective CEI (e.g., by electrolyte additive FEC,[176] or cathode doping agent Li_3PO_4[173]) or HF scavenging (Al_2O_3, CuO).[174]

4.3. SEI-to-CEI Crosstalk

The third major component of a battery cell configuration is the anode, but research on interactive reactions between the two electrodes mostly focusses on cathode and/or CEI to the SEI crosstalk (CEI-to-SEI crosstalk).[197,202–206] Crosstalk from the anode and/or SEI to the CEI on the cathode surface (SEI-to-CEI crosstalk) is less investigated, even though several anode materials like Li metal, Sn, Ge, Ir conversion materials do dissolve in the electrolyte.[207] Published studies reveal a significant influence of the anode material on the CEI characteristics: Zhang et al. conducted a quantitative and systematic XPS analysis to investigate the evolution of the CEI on a $LiCoO_2$ cathode after it was cycled in a battery cell against lithium metal. Authors found that the SEI-to-CEI crosstalk is more prevalent for lithium metal than for carbon graphite anodes and that different SEI components like LiF and Li_2CO_3, travel from electrode to electrode during every charge and discharge process. Increased and continuous SEI formation on lithium metal compared to graphite (or in case of **Figure 11** fresh lithium metal), results in a distinctly different and very much overlooked difference in CEI evolution between LIB and LMB.[178]

Similar results were published by Fang et al. who also used quantitative XPS analysis to investigate the SEI-to-CEI crosstalk between NMC532 and different anode materials (graphite, lithium titanate, and lithium metal). The experimental results showed different, however, always considerable SEI component migration to the CEI, mostly containing LiF, $LiPO_xF_y$, and different organic lithium components ($LiC_xH_yO_z$). It was also shown that the CEI on a cathode material covered by an atomic layer coating of Al_2O_3 displayed a lot fewer SEI components after galvanostatic cycling.[179] Even though few publications cover the phenomenon of SEI-to-CEI crosstalk, the results indicate a clear influence of the anode. More, preferably in situ, research should be conducted on this topic, but it is already imminent that different anode materials pose different requirement to the cathode and utilized electrolyte formulations or otherwise conducted pre-treatment of the cathode.

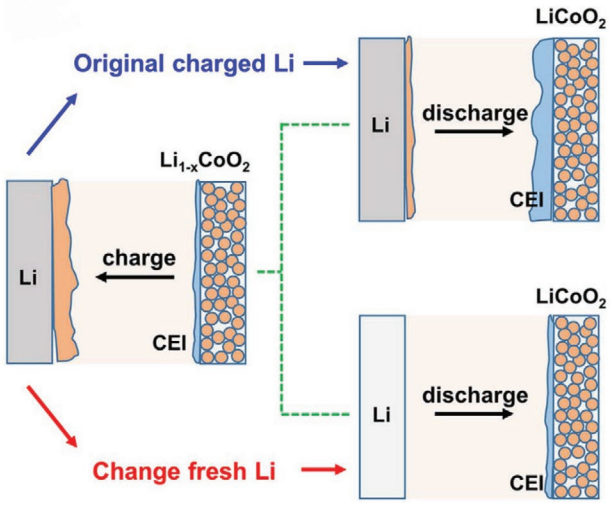

Figure 11. Schematic diagram on the procedure of the verification experiments. In order to investigate the interaction between cathode and anode, Li anode in a $LiCoO_2$||Li battery cell after first charge (4.6 V) was replaced by fresh Li, and the CEI on $LiCoO_2$ after subsequent discharge process was studied and compared with that without interruption. Reproduced with permission.[178] 2018, Elsevier.

4.4. Alternative Cathodes and Electrolyte Formulations

Up to this point, the focus has been set on more conventional manganese/nickel/cobalt containing cathode materials. However, noteworthy research has also been conducted on the CEI on more "exotic" cathode materials: Hestenes et al. used solid state nuclear magnetic resonance spectroscopy, dynamic nuclear polarization (DNP) NMR and EIS measurements to determine the chemical composition of the CEI on a $LiRu_2O_3$ (LRO) cathodes and investigate the SEI-to-CEI cross talk in the LRO–Li setup. Similar chemical components (LiF, Li_2CO_3, PEO) were found as part of the SEI and CEI, once again supporting the proposed SEI-to-CEI crosstalk,[178,179] and determined significant degradation of the CEI during the cathode delithiation step.[180]Another study by Wheatcroft et al. introduces helium ion microscopy (HIM) in combination with in situ TOF-SIMS to investigate the CEI on $LiCoPO_4$. They discovered an inhomogeneous coverage and thickness of the CEI on the cathode surface, leading to local differences regarding resistance and CEI dissolution and deposition behavior, ultimately leading to an ongoing electrolyte consumption on freed up cathode material.[181]

Other publications reported on the enhancing effect of different cathode coatings on the CEI stability.[174,179] However, almost no research has been conducted on the influence of cathode coatings on the CEI. A study by Philipp et al. showed the influence on the CEI by three different coatings on NMC622 cathodes. The coatings were performed with three Lewis acidic metals (Cr_2O_3 > TiO_2 > ZnO; increasing acidity from right to left). EIS and (depth profile) XPS measurement determined, a thinner and more LiF rich containing CEI on the more basic surfaces (ZnO), which is the result of a predominant decomposition of the conducting salts $LiPF_6$. However, against common intuition the more acidic Cr_2O_3 and TiO_2 coated cathodes experiences a better capacity retention than its basic counterpart after 10 cycles. It is proposed, that this is caused by the formation of metal fluorides like CrF_3 and TiF_2 after the initial cycles, which are believed to be more performance promoting than LiF.[182]

All mentioned studies until this point investigated the CEI of lithium-based batteries utilizing organic carbonate-based electrolytes. However, the CEI is also an important factor in aqueous lithium metal batteries, dual ion batteries[208] as well as other alkali metal batteries. Lee et al. used depth profiling XPS and TEM measurements to investigate the CEI on lithium nickel oxide ($LiNiO_2$) cathodes in an aqueous liquid electrolyte and showed how a saturated lithium nitrate ($LiNO_3$) containing electrolyte including LiOH as an additive (pH = 10) will promote the CEI formation during cycling. Besides the inhibited ongoing electrolyte consumption, the formed CEI also prevents transition metal dissolution, as well as reduced hydrogen intercalation compared to a 1 M $LiNO_3$ electrolyte.[190] Targeting a different cathode material, Liu et al. published a study regarding the CEI on a $LiMn_2O_4$ cathode by means of XPS and scanning electrochemical microscopy (SECM) in an aqueous electrolyte. It

was shown, that carbon fluoride polymers and some manganese and lithium salts are the main CEI components and the decomposition of lithium triflate (LiOTf) as the initiating CEI forming reaction was proposed. The formed CEI is able to prevent constant manganese dissolution but also shows increased inhomogeneity after contentious cycling.[191] Finally, the work of Fu et al. deserves recognition who combined XPS, TEM, and Raman measurements as well as operando X-ray absorption spectroscopy (XAS) to correlate the cathode intercalation mechanism and CEI formation/dissolution to the capacity fade of the V_2O_5 cathode for potassium-ion batteries.[192] These few examples show that the investigation of the CEI is an important topic for all different types of cathode materials and battery cell configurations and the power of complementary experimental investigation.

5. Concluding Remarks and Perspective

Electrochemical interfaces and interphases are key components for technologies generating and storing electrical energy. Due to their complexity, these systems are experimentally difficult to study, and research results can drastically vary between different cell chemistry configurations. The (electro-) chemical reactions and related mechanisms regarding the CEI are still far from being well understood and pose a major hurdle for research efforts in tailored design of electrolyte formulations and functional additives. Although many alternatives are described in literature, there are still no clear winners or favored paths toward the ultimate goal of designing and developing controllable positive electrode-liquid electrolyte interphases. Systematic research and enhanced understanding of the (electro)chemistry of both, the CEI as well as the processes at the interface and of the interphase toward the cathode and the electrolyte, with a focus on the composition, morphology, and dynamics of the CEI represent the first steps toward target-oriented interface and electrolyte design, enabling development of high-performance Li-based batteries with high energy, high Coulombic/voltage efficiency (= energy efficiency) and capacity retention over a long lifetime.

Acknowledgements

The authors kindly acknowledge the financial support within the LILLINT project (13XP0225B) funded by the German Federal Ministry of Education and Research (BMBF). The authors also kindly acknowledge the support by European Union's Horizon 2020 research and innovation program under grant agreement No. 957213.

Open access funding enabled and organized by Projekt DEAL.

Conflict of Interest

The authors declare no conflict of interest.

Keywords

cathode electrolyte interphase, CEI, functional additives, liquid electrolytes, lithium-based batteries

Received: October 22, 2021
Revised: November 11, 2021
Published online: January 2, 2022

[1] J. Kasnatscheew, R. Wagner, M. Winter, I. C. Laskovic, in *Modeling Electrochemical Energy Storage at the Atomic Scale*, Springer International Publishing, New York **2018**, pp. 23–51.
[2] Z. J. Xu, *Nano-Micro Lett.* **2018**, *10*, 1.
[3] K. Xu, A. Von Cresce, *J. Mater. Chem.* **2011**, *21*, 9849.
[4] H. R. Luckarift, P. Atanassov, G. R. Johnson, *Enzymatic Fuel Cells: From Fundamentals to Applications*, Wiley, New York **2014**.
[5] K. Xu, in *Encyclopedia of Electrochemical Power Sources*, Elsevier, New York **2009**, pp. 51–70.
[6] M. Gauthier, T. J. Carney, A. Grimaud, L. Giordano, N. Pour, H. H. Chang, D. P. Fenning, S. F. Lux, O. Paschos, C. Bauer, F. Maglia, S. Lupart, P. Lamp, Y. Shao-Horn, *J. Phys. Chem. Lett.* **2015**, *6*, 4653.
[7] E. Peled, S. Menkin, *J. Electrochem. Soc.* **2017**, *164*, A1703.
[8] B. Horstmann, J. Shi, R. Amine, M. Werres, X. He, H. Jia, F. Hausen, I. Cekic-Laskovic, S. Wiemers-Meyer, J. Lopez, D. Galvez-Aranda, F. Baakes, D. Bresser, C.-C. Su, Y. Xu, W. Xu, P. Jakes, R.-A. Eichel, E. Figgemeier, U. Krewer, J. M. Seminario, P. B. Balbuena, C. Wang, S. Passerini, Y. Shao-Horn, M. Winter, K. Amine, R. Kostecki, A. Latz, *Energy Environ. Sci.* **2021**, *14*, 5289.
[9] F. M. Weber, I. Kohlhaas, E. Figgemeier, *J. Electrochem. Soc.* **2020**, *167*, 140523.
[10] I. Cekic-Laskovic, N. Von Aspern, L. Imholt, S. Kaymaksiz, K. Oldiges, *Top. Curr. Chem.* **2017**, *375*, 37.
[11] E. Peled, H. Yamin, *Isr. J. Chem.* **1979**, *18*, 131.
[12] D. R. Gallus, R. Wagner, S. Wiemers-Meyer, M. Winter, I. Cekic-Laskovic, *Electrochim. Acta* **2015**, *184*, 410.
[13] M. Weiss, F. J. Simon, M. R. Busche, T. Nakamura, D. Schröder, F. H. Richter, J. Janek, *Electrochem. Energy Rev.* **2020**, *3*, 221.
[14] N.-S. Choi, J.-G. Han, S.-Y. Ha, I. Park, C.-K. Back, *RSC Adv.* **2015**, *5*, 2732.
[15] A. Würsig, H. Buqa, M. Holzapfel, F. Krumeich, P. Novák, *Electrochem. Solid-State Lett.* **2005**, *8*, A34.
[16] K. Edström, T. Gustafsson, J. O. Thomas, *Electrochim. Acta* **2004**, *50*, 397.
[17] Y. Wu, X. Liu, L. Wang, X. Feng, D. Ren, Y. Li, X. Rui, Y. Wang, X. Han, G. L. Xu, H. Wang, L. Lu, X. He, K. Amine, M. Ouyang, *Energy Storage Mater.* **2021**, *37*, 77.
[18] A. Manthiram, *Nat. Commun.* **2020**, *11*, 1550.
[19] D. Zhao, S. Li, *Front. Chem.* **2020**, *8*, 1.
[20] H. Wang, X. Li, F. Li, X. Liu, S. Yang, J. Ma, *Electrochem. Commun.* **2021**, *122*, 106870.
[21] X. Yu, A. Manthiram, *Energy Environ. Sci.* **2018**, *11*, 527.
[22] C. Yan, R. Xu, Y. Xiao, J. F. Ding, L. Xu, B. Q. Li, J. Q. Huang, *Adv. Funct. Mater.* **2020**, *30*, 1909887.
[23] W. Guo, Y. Meng, Y. Hu, X. Wu, Z. Ju, Q. Zhuang, *Front. Energy Res.* **2020**, *8*, 170.
[24] R. Hausbrand, *J. Chem. Phys.* **2020**, *152*, 180902.
[25] A. Wang, S. Kadam, H. Li, S. Shi, Y. Qi, *npj Comput. Mater.* **2018**, *4*, 15.
[26] B. Horstmann, F. Single, A. Latz, *Curr. Opin. Electrochem.* **2019**, *13*, 61.
[27] S. Phul, A. Deshpande, B. Krishnamurthy, *Electrochim. Acta* **2015**, *164*, 281.
[28] F. Ospina-Acevedo, N. Guo, P. B. Balbuena, *J. Mater. Chem. A* **2020**, *8*, 17036.
[29] N. G. Hörmann, O. Andreussi, N. Marzari, *J. Chem. Phys.* **2019**, *150*, 041730.
[30] Z. Ahmad, V. Venturi, H. Hafiz, V. Viswanathan, *J. Phys. Chem. C* **2021**, *125*, 11301.
[31] I. E. Castelli, M. Zorko, T. M. Østergaard, P. F. B. D. Martins, P. P. Lopes, B. K. Antonopoulos, F. Maglia, N. M. Markovic, D. Strmcnik, J. Rossmeisl, *Chem. Sci.* **2020**, *11*, 3914.
[32] Z. Chen, L. Ryzhik, D. Palanker, *Phys. Rev. Appl.* **2020**, *13*, 014004.
[33] M. Winter, *Z. Phys. Chem.* **2009**, *223*, 1395.
[34] J. Kasnatscheew, B. Streipert, S. Röser, R. Wagner, I. Cekic-Laskovic, M. Winter, *Phys. Chem. Chem. Phys.* **2017**, *19*, 16078.
[35] G. Zampardi, F. L. Mantia, *Batteries Supercaps* **2020**, *3*, 672.

[36] Y. Xie, H. Gao, J. Gim, A. T. Ngo, Z. F. Ma, Z. Chen, *J. Phys. Chem. Lett.* **2019**, *10*, 589.
[37] G. V. Zhuang, G. Chen, J. Shim, X. Song, P. N. Ross, T. J. Richardson, *J. Power Sources* **2004**, *134*, 293.
[38] K. Matsumoto, R. Kuzuo, K. Takeya, A. Yamanaka, *J. Power Sources* **1999**, *81–82*, 558.
[39] D. Aurbach, M. D. Levi, E. Levi, H. Teller, B. Markovsky, G. Salitra, U. Heider, L. Heider, *J. Electrochem. Soc.* **1998**, *145*, 3024.
[40] J. Kim, Y. Hong, K. S. Ryu, M. G. Kim, J. Cho, *Electrochem. Solid-State Lett.* **2005**, *9*, A19.
[41] Y. Arinicheva, M. Wolff, S. Lobe, C. Dellen, D. Fattakhova-Rohlfing, O. Guillon, D. Böhm, F. Zoller, R. Schmuch, J. Li, M. Winter, E. Adamczyk, V. Pralong, in *Advanced Ceramics for Energy Conversion and Storage*, Elsevier, New York **2019**, pp. 549–709.
[42] Y. Bi, T. Wang, M. Liu, R. Du, W. Yang, Z. Liu, Z. Peng, Y. Liu, D. Wang, X. Sun, *RSC Adv.* **2016**, *6*, 19233.
[43] A. T. S. Freiberg, J. Sicklinger, S. Solchenbach, H. A. Gasteiger, *Electrochim. Acta* **2020**, *346*, 136271.
[44] M. M. Besli, C. Usubelli, M. Metzger, V. Pande, K. Harry, D. Nordlund, S. Sainio, J. Christensen, M. M. Doeff, S. Kuppan, *ACS Appl. Mater. Interfaces* **2020**, *12*, 20605.
[45] X. Qi, B. Blizanac, A. Dupasquier, A. Lal, P. Niehoff, T. Placke, M. Oljaca, J. Li, M. Winter, **2015**, *162*, 339.
[46] K. Xu, S. P. Ding, T. R. Jow, *J. Electrochem. Soc.* **1999**, *146*, 4172.
[47] M. Egashira, H. Takahashi, S. Okada, J. I. Yamaki, *J. Power Sources* **2001**, *92*, 267.
[48] R. V. Chebiam, A. M. Kannan, F. Prado, A. Manthiram, *Electrochem. Commun.* **2001**, *3*, 624.
[49] K. Hayashi, Y. Nemoto, S. I. Tobishima, J. I. Yamaki, *Electrochim. Acta* **1999**, *44*, 2337.
[50] B. L. D. Rinkel, D. S. Hall, I. Temprano, C. P. Grey, *J. Am. Chem. Soc.* **2020**, *142*, 15058.
[51] X. Qi, B. Blizanac, A. Dupasquier, P. Meister, T. Placke, *Phys. Chem. Chem. Phys.* **2014**, *16*, 25306.
[52] T. Placke, A. Heckmann, R. Schmuch, P. Meister, K. Beltrop, M. Winter, *Joule* **2018**, *2*, 2528.
[53] A. Manthiram, *J. Phys. Chem. Lett.* **2011**, *2*, 176.
[54] J. B. Goodenough, Y. Kim, *Chem. Mater.* **2010**, *22*, 587.
[55] M. Hu, X. Pang, Z. Zhou, *J. Power Sources* **2013**, *237*, 229.
[56] S. Tan, Y. J. Ji, Z. R. Zhang, Y. Yang, *ChemPhysChem* **2014**, *15*, 1956.
[57] P. Hilbig, L. Ibing, B. Streipert, R. Wagner, M. Winter, I. Cekic-Laskovic, *Curr. Top. Electrochem.* **2018**, *20*, 1.
[58] P. Isken, C. Dippel, R. Schmitz, R. W. Schmitz, M. Kunze, S. Passerini, M. Winter, *Electrochim. Acta* **2011**, *56*, 7530.
[59] A. Manthiram, T. Muraliganth, *Handbook of Battery Materials*, Wiley VCH Verlag, GmBH & Co KG, Weinheim **2011**.
[60] P. Handel, G. Fauler, K. Kapper, M. Schmuck, C. Stangl, R. Fischer, F. Uhlig, S. Koller, *J. Power Sources* **2014**, *267*, 255.
[61] P. K. Nayak, J. Grinblat, M. Levi, Y. Wu, B. Powell, D. Aurbach, *J. Electroanal. Chem.* **2014**, *733*, 6.
[62] P. Yan, J. Zheng, M. Gu, J. Xiao, J. G. Zhang, C. M. Wang, *Nat. Commun.* **2017**, *8*, 14101.
[63] S. K. Jung, H. Gwon, J. Hong, K. Y. Park, D. H. Seo, H. Kim, J. Hyun, W. Yang, K. Kang, *Adv. Energy Mater.* **2014**, *4*, 1300787.
[64] F. L. Mantia, F. Rosciano, N. Tran, P. Novák, *J. Electrochem. Soc.* **2009**, *156*, A823.
[65] P. Aurora, R. E. White, M. Doyle, P. Arora, R. E. White, M. Doyle, *J. Electrochem. Soc.* **1998**, *145*, 3647.
[66] R. Wagner, M. Korth, B. Streipert, J. Kasnatscheew, D. R. Gallus, S. Brox, M. Amereller, I. Cekic-Laskovic, M. Winter, *ACS Appl. Mater. Interfaces* **2016**, *8*, 30871.
[67] R. Wagner, B. Streipert, V. Kraft, A. R. Jiménez, S. Röser, J. Kasnatscheew, D. R. Gallus, M. Börner, C. Mayer, H. F. Arlinghaus, M. Korth, M. Amereller, I. Cekic-Laskovic, M. Winter, *Adv. Mater. Interfaces* **2016**, *3*, 1600096.
[68] J. Kasnatscheew, U. Rodehorst, B. Streipert, S. Wiemers-meyer, R. Jakelski, R. Wagner, I. Cekic-Laskovic, M. Winter, *J. Electrochem. Soc.* **2016**, *163*, A2943.
[69] J. Kasnatscheew, M. Evertz, B. Streipert, R. Wagner, R. Klöpsch, B. Vortmann, H. Hahn, S. Nowak, M. Amereller, A.-C. Gentschev, P. Lamp, M. Winter, *Phys. Chem. Chem. Phys.* **2016**, *18*, 3956.
[70] F. Lin, I. M. Markus, D. Nordlund, T. C. Weng, M. D. Asta, H. L. Xin, M. M. Doeff, *Nat. Commun.* **2014**, *5*, 3529.
[71] B. Strehle, K. Kleiner, R. Jung, F. Chesneau, M. Mendez, H. A. Gasteiger, M. Piana, *J. Electrochem. Soc.* **2017**, *164*, A400.
[72] D. Leanza, M. Mirolo, C. A. F. Vaz, P. Novák, M. El Kazzi, *Batteries Supercaps* **2019**, *2*, 482.
[73] H. Zheng, Q. Sun, G. Liu, X. Song, V. S. Battaglia, *J. Power Sources* **2012**, *207*, 134.
[74] J. Wandt, A. T. S. Freiberg, A. Ogrodnik, H. A. Gasteigner, *Mater. Today* **2018**, *21*, 825.
[75] O. Borodin, M. Olguin, C. E. Spear, K. W. Leiter, J. Knap, *Nanotechnology* **2015**, *26*, 354003.
[76] A. J. Bard, L. R. Faulkner, *Electrochemical Methods: Fundamentals and Applications*, Wiley, New York **2000**.
[77] E. R. Fadel, F. Faglioni, G. Samsonidze, N. Molinari, B. V. Merinov, W. A. Goddard, J. C. Grossman, J. P. Mailoa, B. Kozinsky, *Nat. Commun.* **2019**, *10*, 3360.
[78] X. Ren, P. Gao, L. Zou, S. Jiao, X. Cao, X. Zhang, H. Jia, M. H. Engelhard, B. E. Matthews, H. Wu, H. Lee, C. Niu, C. Wang, B. W. Arey, J. Xiao, J. Liu, J. G. Zhang, W. Xu, *Proc. Natl. Acad. Sci. U. S. A.* **2020**, *117*, 28603.
[79] I. Popov, R. L. Sacci, N. C. Sanders, R. A. Matsumoto, M. W. Thompson, N. C. Osti, T. Kobayashi, M. Tyagi, E. Mamontov, M. Pruski, P. T. Cummings, A. P. Sokolov, *J. Phys. Chem. C* **2020**, *124*, 8457.
[80] S. Feng, M. Huang, J. R. Lamb, W. Zhang, R. Tatara, Y. Zhang, Y. Guang Zhu, C. F. Perkinson, J. A. Johnson, Y. Shao-Horn, *Chem* **2019**, *5*, 2630.
[81] D. Aurbach, K. Gamolsky, B. Markovsky, G. Salitra, Y. Gofer, U. Heider, R. Östen, M. Schmidt, *J. Electrochem. Soc.* **2000**, *147*, 1322.
[82] D. Aurbach, B. Markovsky, A. Rodkin, E. Levi, Y. S. Cohen, H. J. Kim, M. Schmidt, *Electrochim. Acta* **2002**, *47*, 4291.
[83] K. Leung, *J. Phys. Chem. C* **2012**, *116*, 9852.
[84] S. Xu, G. Luo, R. Jacobs, S. Fang, M. K. Mahanthappa, R. J. Hamers, D. Morgan, *ACS Appl. Mater. Interfaces* **2017**, *9*, 20545.
[85] Y. Zhang, Y. Katayama, R. Tatara, L. Giordano, Y. Yu, D. Fraggedakis, J. G. Sun, F. Maglia, R. Jung, M. Z. Bazant, Y. Shao-Horn, *Energy Environ. Sci.* **2020**, *13*, 183.
[86] X. T. Wang, Z. Y. Gu, W. H. Li, X. X. Zhao, J. Z. Guo, K. Di Du, X. X. Luo, X. L. Wu, *Chem. - Asian J.* **2020**, *15*, 2803.
[87] C. L. Campion, W. Li, B. L. Lucht, *J. Electrochem. Soc.* **2005**, *152*, A2327.
[88] Z. Chen, K. Amine, *Electrochem. Commun.* **2007**, *9*, 703.
[89] A. Tornheim, M. He, C.-C. Su, Z. Zhang, *J. Electrochem. Soc.* **2017**, *164*, A6366.
[90] L. Imholt, S. Röser, M. Börner, B. Streipert, B. R. Rad, M. Winter, I. Cekic-Laskovic, *Electrochim. Acta* **2017**, *235*, 332.
[91] R. Chen, F. Liu, Y. Chen, Y. Ye, Y. Huang, F. Wu, L. Li, *J. Power Sources* **2016**, *306*, 70.
[92] P. Hong, M. Xu, X. Zheng, Y. Zhu, Y. Liao, L. Xing, Q. Huang, H. Wan, Y. Yang, W. Li, *J. Power Sources* **2016**, *329*, 216.
[93] Y. M. Song, C. K. Kim, K. E. Kim, S. Y. Hong, N. S. Choi, *J. Power Sources* **2016**, *302*, 22.
[94] X. Zheng, T. Huang, Y. Pan, W. Wang, G. Fang, K. Ding, M. Wu, *ACS Appl. Mater. Interfaces* **2017**, *9*, 18758.
[95] F. M. Wang, S. A. Pradanawati, N. H. Yeh, S. C. Chang, Y. T. Yang, S. H. Huang, P. L. Lin, J. F. Lee, H. S. Sheu, M. L. Lu, C. K. Chang, A. Ramar, C. H. Su, *Chem. Mater.* **2017**, *29*, 5537.

[96] J. Chen, H. Zhang, M. Wang, J. Liu, C. Li, P. Zhang, *J. Power Sources* **2016**, *303*, 41.
[97] J. Li, L. Xing, R. Zhang, M. Chen, Z. Wang, M. Xu, W. Li, *J. Power Sources* **2015**, *285*, 360.
[98] X. Wang, L. Xing, X. Liao, X. Chen, W. Huang, Q. Yu, M. Xu, Q. Huang, W. Li, *Electrochim. Acta* **2015**, *173*, 804.
[99] Z. Wang, L. Xing, J. H. Li, M. Xu, W. Li, *J. Power Sources* **2016**, *307*, 587.
[100] X. Qi, L. Tao, H. Hahn, C. Schultz, D. R. Gallus, X. Cao, S. Nowak, S. Röser, J. Li, I. Cekic-Laskovic, B. R. Rad, M. Winter, *RSC Adv.* **2016**, *6*, 38342.
[101] J. Xu, Q. Xia, F. Chen, T. Liu, L. Li, X. Cheng, W. Lu, X. Wu, *Electrochim. Acta* **2016**, *191*, 687.
[102] Y. K. Han, J. Yoo, T. Yim, *J. Mater. Chem. A* **2015**, *3*, 10900.
[103] Z. Zhou, Y. Ma, L. Wang, P. Zuo, X. Cheng, C. Du, G. Yin, Y. Gao, *Electrochim. Acta* **2016**, *216*, 44.
[104] L. Wang, Y. Ma, Q. Li, Y. Cui, P. Wang, X. Cheng, P. Zuo, C. Du, Y. Gao, G. Yin, *Electrochim. Acta* **2017**, *243*, 72.
[105] N. Xu, Y. Sun, J. Shi, J. Chen, G. Liu, K. Zhou, H. He, J. Zhu, Z. Zhang, Y. Yang, *J. Power Sources* **2021**, *511*, 230437.
[106] F. An, H. Zhao, W. Zhou, Y. Ma, P. Li, *Sci. Rep.* **2019**, *9*, 14108.
[107] S. H. Lim, W. Cho, Y. J. Kim, T. Yim, *J. Power Sources* **2016**, *336*, 465.
[108] L. Xia, Y. Xia, Z. Liu, *J. Power Sources* **2015**, *278*, 190.
[109] H. Cai, H. Jing, X. Zhang, M. Shen, Q. Wang, *J. Electrochem. Soc.* **2017**, *164*, A714.
[110] K. Wang, L. Xing, Y. Zhu, X. Zheng, D. Cai, W. Li, *J. Power Sources* **2017**, *342*, 677.
[111] Y. Ji, P. Zhang, M. Lin, W. Zhao, Z. Zhang, Y. Zhao, Y. Yang, *J. Power Sources* **2017**, *359*, 391.
[112] P. Janssen, B. Streipert, R. Krafft, P. Murmann, R. Wagner, L. Lewis-Alleyne, G.-V. Röschenthaler, M. Winter, I. Cekic-Laskovic, *J. Power Sources* **2017**, *367*, 72.
[113] T. J. Lee, J. B. Lee, T. Yoon, D. Kim, O. B. Chae, J. Jung, J. Soon, J. Heon Ryu, J. J. Kim, S. M. Oh, J. H. Ryu, J. J. Kim, S. M. Oh, *J. Electrochem. Soc.* **2016**, *163*, A898.
[114] Y. Zhu, Y. Li, M. Bettge, D. P. Abraham, *J. Electrochem. Soc.* **2012**, *159*, A2109.
[115] S. Y. Ha, J. G. Han, Y. M. Song, M. J. Chun, S. Il Han, W. C. Shin, N. S. Choi, *Electrochim. Acta* **2013**, *104*, 170.
[116] M. Xu, L. Zhou, Y. Dong, U. Tottempudi, J. Demeaux, A. Garsuch, B. L. Lucht, *ECS Electrochem. Lett.* **2015**, *4*, A83.
[117] Y. Kaneko, J. Park, H. Yokotsuji, M. Odawara, H. Takase, M. Ue, M. E. Lee, *Electrochim. Acta* **2016**, *222*, 271.
[118] Y. Dong, B. T. Young, Y. Zhang, T. Yoon, D. R. Heskett, Y. Hu, B. L. Lucht, *ACS Appl. Mater. Interfaces* **2017**, *9*, 20467.
[119] M. Xu, L. Zhou, Y. Dong, Y. Chen, J. Demeaux, A. D. MacIntosh, A. Garsuch, B. L. Lucht, *Energy Environ. Sci.* **2016**, *9*, 1308.
[120] Y. Li, B. Cheng, F. Jiao, K. Wu, *ACS Appl. Mater. Interfaces* **2020**, *12*, 16298.
[121] X. Wang, S. Li, W. Zhang, D. Wang, Z. Shen, J. Zheng, H. L. Zhuang, Y. He, Y. Lu, *Nano Energy* **2021**, *89*, 106353.
[122] X. Zheng, T. Huang, Y. Pan, W. Wang, G. Fang, M. Wu, *J. Power Sources* **2015**, *293*, 196.
[123] Y. S. Kang, M. S. Park, I. Park, D. Y. Kim, J. H. Park, K. Park, M. Koh, S. G. Doo, *ACS Appl. Mater. Interfaces* **2017**, *9*, 3590.
[124] Y. Dong, J. Demeaux, Y. Zhang, M. Xu, L. Zhou, A. D. MacIntosh, B. L. Lucht, *J. Electrochem. Soc.* **2017**, *164*, A128.
[125] L. Wang, Y. Ma, Q. Li, Z. Zhou, X. Cheng, P. Zuo, C. Du, Y. Gao, G. Yin, *J. Power Sources* **2017**, *361*, 227.
[126] H. Rong, M. Xu, Y. Zhu, B. Xie, H. Lin, Y. Liao, L. Xing, W. Li, *J. Power Sources* **2016**, *332*, 312.
[127] A. M. Haregewoin, A. S. Wotango, B. J. Hwang, *Energy Environ. Sci.* **2016**, *9*, 1955.
[128] N. Von Aspern, S. Röser, B. Rezaei Rad, P. Murmann, B. Streipert, X. Mönnighoff, S. D. Tillmann, M. Shevchuk, O. Stubbmann-Kazakova, G. V. Röschenthaler, S. Nowak, M. Winter, I. Cekic-Laskovic, B. R. Rad, P. Murmann, B. Streipert, X. Mönnighoff, S. D. Tillmann, M. Shevchuk, O. Stubbmann-Kazakova, G. V. Röschenthaler, S. Nowak, M. Winter, I. Cekic-Laskovic, *J. Fluorine Chem.* **2017**, *198*, 24.
[129] X. Zheng, T. Huang, Y. Pan, W. Wang, G. Fang, K. Ding, M. Wu, *J. Power Sources* **2016**, *319*, 116.
[130] N. von Aspern, M. Leissing, C. Wölke, D. Diddens, T. Kobayashi, M. Börner, O. Stubbmann-Kazakova, V. Kozel, G. V. Röschenthaler, J. Smiatek, S. Nowak, M. Winter, I. Cekic-Laskovic, *ChemElectroChem* **2020**, *7*, 1499.
[131] T. Placke, O. Fromm, S. F. Lux, P. Bieker, S. Rothermel, H.-W. Meyer, S. Passerini, M. Winter, *J. Electrochem. Soc.* **2012**, *159*, A1755.
[132] X. Fan, L. Chen, X. Ji, T. Deng, S. Hou, J. Chen, J. Zheng, F. Wang, J. Jiang, K. Xu, C. Wang, *Chem* **2018**, *4*, 174.
[133] N. von Aspern, G.-V. Röschenthaler, M. Winter, I. Cekic-Laskovic, *Angew. Chem., Int. Ed.* **2019**, *58*, 15978.
[134] L. Xia, H. Miao, C. Zhang, G. Z. Chen, J. Yuan, *Energy Storage Mater.* **2021**, *38*, 542.
[135] T. Böttcher, N. Kalinovich, O. Kazakova, M. Ponomarenko, K. Vlasov, M. Winter, G. V. Röschenthaler, in *Advanced Fluoride-Based Materials for Energy Conversion*, Elsevier, Amsterdam **2015**, pp. 125–145.
[136] T. Böttcher, B. Duda, N. Kalinovich, O. Kazakova, M. Ponomarenko, K. Vlasov, *Prog. Solid State Chem.* **2014**, *42*, 202.
[137] J. Besenhard, K. v. Werner, M. Winter, *DE 196191233 A1*, **1997**.
[138] Y. Okuno, K. Ushirogata, K. Sodeyama, Y. Tateyama, *Phys. Chem. Chem. Phys.* **2016**, *18*, 8643.
[139] M. He, C. C. Su, C. Peebles, Z. Feng, J. G. Connell, C. Liao, Y. Wang, I. A. Shkrob, Z. Zhang, *ACS Appl. Mater. Interfaces* **2016**, *8*, 11450.
[140] N. L. Hamidah, G. Nugroho, F. M. Wang, *Ionics* **2016**, *22*, 33.
[141] J. Xia, R. Petibon, A. Xiao, W. M. Lamanna, J. R. Dahn, *J. Electrochem. Soc.* **2016**, *163*, A1637.
[142] J. Mun, J. Lee, T. Hwang, J. Lee, H. Noh, W. Choi, *J. Electroanal. Chem.* **2015**, *745*, 8.
[143] J. G. Han, J. Bin Lee, A. Cha, T. K. Lee, W. Cho, S. Chae, S. J. Kang, S. K. Kwak, J. Cho, S. Y. Hong, N. S. Choi, *Energy Environ. Sci.* **2018**, *11*, 1552.
[144] N. von Aspern, M. Grünebaum, D. Diddens, T. Pollard, C. Wölke, O. Borodin, M. Winter, I. Cekic-Laskovic, *J. Power Sources* **2020**, *461*, 228159.
[145] C. Wölke, D. Diddens, B. Heidrich, M. Winter, I. Cekic-Laskovic, *ChemElectroChem* **2021**, *8*, 972.
[146] P. Murmann, M. Xaver, N. Von Aspern, P. Janssen, N. Kalinovich, M. Shevchuk, O. Kazakova, R. Gerd-volker, *J. Electrochem. Soc.* **2016**, *163*, A751.
[147] N. von Aspern, S. Röser, B. Rezaei Rad, P. Murmann, B. Streipert, X. Mönnighoff, S. D. Tillmann, M. Shevchuk, O. Stubbmann-Kazakova, G. V. Röschenthaler, S. Nowak, M. Winter, I. Cekic-Laskovic, *J. Fluorine Chem.* **2017**, *198*, 24.
[148] X. Zhang, X. Cheng, X. Chen, C. Yan, Q. Zhang, *Adv. Funct. Mater.* **2017**, *27*, 1605989.
[149] N. von Aspern, C. Wölke, M. Börner, M. Winter, I. Cekic-Laskovic, *J. Solid State Electrochem.* **2020**, *24*, 3145.
[150] N. Von Aspern, D. Diddens, T. Kobayashi, M. Börner, O. Stubbmann-Kazakova, V. Kozel, G. V. Röschenthaler, J. Smiatek, M. Winter, I. Cekic-Laskovic, *ACS Appl. Mater. Interfaces* **2019**, *11*, 16605.
[151] J. Cha, J. G. Han, J. Hwang, J. Cho, N. S. Choi, *J. Power Sources* **2017**, *357*, 97.
[152] H. Gao, F. Maglia, P. Lamp, K. Amine, Z. Chen, *ACS Appl. Mater. Interfaces* **2017**, *9*, 44542.
[153] W. Huang, L. Xing, R. Zhang, X. Wang, W. Li, *J. Power Sources* **2015**, *293*, 71.
[154] N. Xu, J. Shi, G. Liu, X. Yang, J. Zheng, Z. Zhang, Y. Yang, *J. Power Sources Adv.* **2021**, *7*, 100043.

[155] H. Wang, D. Sun, X. Li, W. Ge, B. Deng, M. Qu, G. Peng, *Electrochim. Acta* **2017**, *254*, 112.
[156] A. Kazzazi, D. Bresser, M. Kuenzel, M. Hekmatfar, J. Schnaidt, Z. Jusys, T. Diemant, R. J. Behm, M. Copley, K. Maranski, J. Cookson, I. de Meatza, P. Axmann, M. Wohlfahrt-Mehrens, S. Passerini, *J. Power Sources* **2021**, *482*, 228975.
[157] P. Janssen, J. Kasnatscheew, B. Streipert, C. Wendt, P. Murmann, M. Ponomarenko, O. Stubbmann-Kazakova, G.-V. Röschenthaler, M. Winter, I. Cekic-Laskovic, *J. Electrochem. Soc.* **2018**, *165*, A3525.
[158] T. Yang, H. Zeng, W. Wang, X. Zhao, W. Fan, C. Wang, X. Zuo, R. Zeng, J. Nan, *J. Mater. Chem. A* **2019**, *7*, 8292.
[159] D. Aurbach, B. Markovsky, G. Salitra, E. Markevich, Y. Talyossef, M. Koltypin, L. Nazar, B. Ellis, D. Kovacheva, *J. Power Sources* **2007**, *165*, 491.
[160] H. Sclar, D. Kovacheva, E. Zhecheva, R. Stoyanova, R. Lavi, G. Kimmel, J. Grinblat, O. Girshevitz, F. Amalraj, O. Haik, *J. Electrochem. Soc.* **2009**, *156*, A938.
[161] K. J. Carroll, M. C. Yang, G. M. Veith, N. J. Dudney, Y. S. Meng, *Electrochem. Solid-State Lett.* **2012**, *15*, 88.
[162] T. R. Jow, K. Xu, O. Borodin, M. Ue, *Electrolytes for Lithium & Lithium-Ion Batteries*, Springer, New York **2014**.
[163] Y. Park, S. H. Shin, S. M. Lee, S. P. Kim, H. C. Choi, Y. M. Jung, *J. Mol. Struct.* **2014**, *1069*, 183.
[164] R. Scipioni, D. Isheim, S. A. Barnett, *Appl. Mater. Today* **2020**, *20*, 100748.
[165] M. Mao, B. Huang, Q. Li, C. Wang, Y.-B. He, F. Kang, *Nano Energy* **2020**, *78*, 105282.
[166] Z. Zhang, J. Yang, W. Huang, H. Wang, W. Zhou, Y. Li, Y. Li, J. Xu, W. Huang, W. Chiu, Y. Cui, *Matter* **2021**, *4*, 302.
[167] Y. Meng, G. Chen, L. Shi, H. Liu, D. Zhang, *ACS Appl. Mater. Interfaces* **2019**, *11*, 45108.
[168] Z. W. Yin, X. X. Peng, J. T. Li, C. H. Shen, Y. P. Deng, Z. G. Wu, T. Zhang, Q. B. Zhang, Y. X. Mo, K. Wang, L. Huang, H. Zheng, S. G. Sun, *ACS Appl. Mater. Interfaces* **2019**, *11*, 16214.
[169] I. Takahashi, H. Kiuchi, A. Ohma, T. Fukunaga, E. Matsubara, *J. Phys. Chem. C* **2020**, *124*, 9243.
[170] W. Lu, J. Zhang, J. Xu, X. Wu, L. Chen, *ACS Appl. Mater. Interfaces* **2017**, *9*, 19313.
[171] Q. Li, Y. Wang, X. Wang, X. Sun, J. N. Zhang, X. Yu, H. Li, *ACS Appl. Mater. Interfaces* **2020**, *12*, 2319.
[172] E. M. Erickson, W. Li, A. Dolocan, A. Manthiram, *ACS Appl. Mater. Interfaces* **2020**, *12*, 16451.
[173] F. Wu, W. Li, L. Chen, Y. Su, L. Bao, W. Bao, Z. Yang, J. Wang, Y. Lu, S. Chen, *Energy Storage Mater.* **2020**, *28*, 383.
[174] T. Yoon, J. Soon, T. Jin Lee, J. Heon Ryu, S. M. Oh, *J. Power Sources* **2021**, *503*, 230051.
[175] W. Wang, Q. Yang, K. Qian, B. Li, *J. Energy Chem.* **2020**, *47*, 72.
[176] Y. Qian, P. Niehoff, M. Börner, M. Grützke, X. Mönnighoff, P. Behrends, S. Nowak, M. Winter, F. M. Schappacher, *J. Power Sources* **2016**, *329*, 31.
[177] M. Hekmatfar, I. Hasa, R. Eghbal, D. V. Carvalho, A. Moretti, S. Passerini, *Adv. Mater. Interfaces* **2020**, *7*, 1901500.
[178] J. N. Zhang, Q. Li, Y. Wang, J. Zheng, X. Yu, H. Li, *Energy Storage Mater.* **2018**, *14*, 1.
[179] S. Fang, D. Jackson, M. L. Dreibelbis, T. F. Kuech, R. J. Hamers, *J. Power Sources* **2018**, *373*, 184.
[180] J. C. Hestenes, A. W. Ells, M. Navarro Goldaraz, I. V. Sergeyev, B. Itin, L. E. Marbella, *Front. Chem.* **2020**, *8*, 681.
[181] L. Wheatcroft, N. Klingner, R. Heller, G. Hlawacek, D. Özkaya, J. Cookson, B. J. Inkson, *ACS Appl. Energy Mater.* **2020**, *3*, 8822.
[182] N. D. Phillip, B. L. Armstrong, C. Daniel, G. M. Veith, *ACS Omega* **2020**, *5*, 14968.
[183] X. Zhang, H. Jia, Y. Xu, L. Zou, M. H. Engelhard, B. E. Matthews, C. Wang, J. Zhang, W. Xu, *J. Power Sources Adv.* **2020**, *5*, 100024.
[184] S. Lin, H. Hua, P. Lai, J. Zhao, *Adv. Energy Mater.* **2021**, *11*, 2101775.
[185] S. Lin, H. Hua, Z. Li, J. Zhao, *Appl. Mater. Interfaces* **2020**, *12*, 33710.
[186] Y. Shen, H. Xue, S. Wang, Z. Wang, D. Zhang, D. Yin, L. Wang, Y. Cheng, *J. Colloid Interface Sci.* **2021**, *597*, 334.
[187] W. Li, A. Dolocan, J. Li, Q. Xie, A. Manthiram, *Adv. Energy Mater.* **2019**, *9*, 1901152.
[188] J. Holoubek, M. Yu, S. Yu, M. Li, Z. Wu, D. Xia, P. Bhaladhare, M. S. Gonzalez, T. A. Pascal, P. Liu, Z. Chen, *ACS Energy Lett.* **2020**, *5*, 1438.
[189] X. Zheng, Y. Liao, Z. Zhang, J. Zhu, F. Ren, H. He, Y. Xiang, Y. Zheng, Y. Yang, *J. Energy Chem.* **2020**, *42*, 62.
[190] C. Lee, Y. Yokoyama, Y. Kondo, Y. Miyahara, T. Abe, K. Miyazaki, *Adv. Energy Mater.* **2021**, *11*, 2100756.
[191] S. Liu, D. Liu, S. Wang, X. Cai, K. Qian, F. Kang, B. Li, *J. Mater. Chem. A* **2019**, *7*, 12993.
[192] Q. Fu, A. Sarapulova, L. Zhu, G. Melinte, A. Missyul, E. Welter, X. Luo, M. Knapp, H. Ehrenberg, S. Dsoke, *J. Energy Chem.* **2021**, *62*, 627.
[193] X. chen Bai, G. McMullan, S. H. W. Scheres, *Trends Biochem. Sci.* **2015**, *40*, 49.
[194] Y. Cheng, *Cell* **2015**, *161*, 450.
[195] B. J. Tremolet de Villers, S. Bak, J. Yang, S. Han, *Batteries Supercaps* **2021**, *4*, 778.
[196] W. Zuo, M. Luo, X. Liu, J. Wu, H. Liu, *Energy Environ. Sci.* **2020**, *13*, 4450.
[197] J. Park, D. Kim, D. Jin, C. Phatak, K. Young, Y. Lee, S. Hong, M. Ryou, Y. M. Lee, *J. Power Sources* **2018**, *408*, 136.
[198] M. Wachtler, M. Winter, J. O. Besenhard, *Nano-structured lithium storage alloy anodes. 13th IBA Marrakesh Symposium: Marrakesh (Morocco)*, **1999**; Vol. Abstract No. *24*.
[199] J. Heine, P. Hilbig, X. Qi, P. Niehoff, M. Winter, P. Bieker, *J. Electrochem. Soc.* **2015**, *162*, A1094.
[200] M. Winter, W. K. Appel, B. Evers, T. Hodal, K. Moller, M. Wachtler, M. R. Wagner, G. H. Wrodnigg, J. Besenhard, in *Electroactive Materials*, Springer, Vienna **2001**, pp. 53–66.
[201] S. Nowak, M. Winter, *J. Electrochem. Soc.* **2015**, *162*, A2500.
[202] H. Liu, A. J. Naylor, A. S. Menon, W. R. Brant, K. Edström, R. Younesi, *Adv. Mater. Interfaces* **2020**, *2*, 2000277.
[203] J. Betz, J. P. Brinkmann, R. Nölle, C. Lürenbaum, M. Kolek, M. C. Stan, M. Winter, T. Placke, *Adv. Energy Mater.* **2019**, *9*, 1900574.
[204] O. C. Harris, Y. Lin, Y. Qi, K. Leung, M. H. Tang, *J. Electrochem. Soc.* **2020**, *167*, 013502.
[205] O. C. Harris, K. Leung, M. H. Tang, *J. Electrochem. Soc.* **2020**, *167*, 013503.
[206] T. Joshi, K. Eom, G. Yushin, T. F. Fuller, *J. Electrochem. Soc.* **2014**, *161*, A1915.
[207] H. Jia, R. Kloepsch, X. He, M. Evertz, S. Nowak, J. Li, M. Winter, T. Placke, *Acta Chim. Slov.* **2016**, *63*, 470.
[208] S. Rothermel, P. Meister, G. Schmuelling, O. Fromm, H. Meyer, S. Nowak, M. Winter, T. Placke, *Energy Environ. Sci.* **2014**, *7*, 3412.

Sebastian P. Kühn was born in Bonn, Germany, in 1993. He studied Chemistry at the Rheinische Friedrichs-Wilhelms-University Bonn, and finished his M.Sc. in 2018 (supervisor: Prof. O. Schiemann). He is currently working as a Ph.D. candidate in the group of Prof. Martin Winter at the Helmholtz-Institute Münster (HI MS) "Ionics in Energy Storage" (IEK-12). His research focuses on the characterization and understanding of electrode interphases, their interaction with other battery components and the resulting influences on the battery performance.

Kristina Edström, professor of Inorganic Chemistry at Uppsala University Sweden, coordinates the large-scale European research initiative BATTERY 2030+. She studies Li-ion batteries, Na-ion batteries, solid-state batteries, and other future battery chemistries. She leads the Ångström Advanced Battery Centre. She has more than 280 scientific papers with an H-index of 64. She is elected member of the Royal Academy of Engineering Sciences (IVA), honorary doctor at NTNU, Norway, she received the KTH grand prize, is a Wallenberg Scholar and received the gold medal of IVA. She is the scientific coordinator of Batteries Sweden and trustee in the Faraday Institution, UK.

Martin Winter has been researching in the field of electrochemical energy storage and conversion for 30 years with a focus on the development of new materials, components, and cell designs for batteries and supercapacitors. He currently holds a professorship for "Materials Science, Energy and Electrochemistry" at the Institute of Physical Chemistry at Muenster University, Germany. He is the scientific director of the MEET Battery Research Center at Muenster University and founding director of the Helmholtz-Institute Muenster (HI MS, IEK-12) "Ionics in Energy Storage" an institute branch of Research Center Juelich.

Isidora Cekic-Laskovic obtained a Ph.D. in Physical Organic Chemistry at the Faculty of Physical Chemistry, University of Belgrade. In 2012, she became a research scientist at MEET Battery Research Center and took over the leading responsibility of the research group Electrolyte. Since 2016, she is a research group leader at the Helmholtz-Institute Münster (HI MS, IEK-12) "Ionics in Energy Storage" an institute branch of Research Center Juelich. The main scope of research comprises advanced functional electrolytes for lithium-based battery application from tailored synthesis of novel electrolyte components all the way to interfacial electrochemistry and processes accompanied by high-throughput experimentation.